



Published in final edited form as:

*Nat Biotechnol.* 2021 January ; 39(1): 64–73. doi:10.1038/s41587-020-0613-1.

## Inducible *de novo* expression of neoantigens in tumor cells and mice with NINJA

Martina Damo<sup>1,4</sup>, Brittany Fitzgerald<sup>1,4</sup>, Yisi Lu<sup>2</sup>, Mursal Nader<sup>1</sup>, Ivana William<sup>1</sup>, Julie F. Cheung<sup>1</sup>, Kelli A. Connolly<sup>1</sup>, Gena G. Foster<sup>1</sup>, Elliot Akama-Garren<sup>2</sup>, Da-Yae Lee<sup>2</sup>, Greg P. Chang<sup>2</sup>, Vasilena Gocheva<sup>2</sup>, Leah M. Schmidt<sup>2</sup>, Alice Boileve<sup>2</sup>, Josephine H. Wilson<sup>1</sup>, Can Cui<sup>1</sup>, Isabel Monroy<sup>1</sup>, Prashanth Gokare<sup>1</sup>, Peter Cabeceiras<sup>2</sup>, Tyler Jacks<sup>2,3,5,\*</sup>, Nikhil S. Joshi<sup>1,2,5,\*</sup>

<sup>1</sup>Department of Immunobiology, Yale University School of Medicine, New Haven, CT 06519, USA

<sup>2</sup>Koch Institute for Integrative Cancer Research and Department of Biology, Massachusetts Institute of Technology, Cambridge, MA 02142, USA

<sup>3</sup>Howard Hughes Medical Institute, Massachusetts Institute of Technology, Cambridge, MA 02142, USA

<sup>4</sup>Authors contributed equally to this work

<sup>5</sup>Authors contributed equally to this work

### Abstract

Inducible expression of neoantigens in mice would enable the study of endogenous antigen-specific naïve T cell responses in disease and infection, but has been difficult to generate because leaky antigen expression in the thymus results in central T cell tolerance. Here, we developed iNversion INduced Joined neoAntigen (NINJA), using RNA splicing, DNA recombination, and three levels of regulation to prevent leakiness and allow tight control over neoantigen expression. We apply NINJA to create tumor cell lines with inducible neoantigen expression, which could be used to study anti-tumor immunity. We also show that the genetic regulation in NINJA mice bypasses central and peripheral tolerance mechanisms and allows for robust endogenous CD8 and CD4 T cells responses upon neoantigen induction in peripheral tissues. NINJA will enable studies of how T cells respond to defined neoantigens in the context of peripheral tolerance, transplantation, autoimmune diseases, and cancer.

---

Users may view, print, copy, and download text and data-mine the content in such documents, for the purposes of academic research, subject always to the full Conditions of use:[http://www.nature.com/authors/editorial\\_policies/license.html#terms](http://www.nature.com/authors/editorial_policies/license.html#terms)

\*Corresponding authors.

Author contributions

M.D., B.F., N.S.J. and T.J. designed research. M.D., B.F., Y.L., M.N., I.W., J.F.C., K.A.C., G.G.F., E.A.-G., D.L., G.P.C., V.G., L.M.S., A.B., J.H.W., C.C., I.M., P.G., and P.C. performed research. M.D., B.F. and N.D.J. analyzed data and wrote the manuscript.

Competing interests

The authors declare no financial and/or non-financial competing interests in relation to the work described.

Supplementary Information

Supplementary Information including Tables and Notes is available for this manuscript.

Data availability

The authors declare that the data supporting the findings of this study are available within the paper, its Extended Data Figures and Supplementary Material.

## Main

Investigating how endogenous T cell responses are modulated following antigen encounter is at the core of multiple areas of immunobiology. T cells encounter antigens in a variety of different contexts, including exposure to viral/bacterial antigens during infection, tumor neoantigens in developing cancers, mismatched organs following transplantation, and self/commensal antigens under physiological conditions. The outcome of these encounters can range from potent effector responses to antigen-specific tolerance and is determined by the parameters of the challenge (inflammation, antigen-strength, TCR avidity, antigen chronicity, *etc.*)<sup>1–5</sup>. To understand the precise mechanisms by which these outcomes are dictated, immunologists require model systems where T cell responses can be compared directly between experimental challenges (*i.e.*, virus, bacteria, and tumors expressing the same model antigen).

To introduce model antigens into a tissue or cell type of interest, researchers have developed experimental systems aimed at achieving robust control over when and/or where antigens are expressed and presented. These include the use of (1) genetic models such as tissue-specific promoters (which control antigen location but are expressed constitutively) or inducible neoantigen models (which rely on genetic elements to suppress unwanted promoter activity prior to induction)<sup>6–12</sup> and (2) methods for tissue- or cell-specific antigen delivery (which allow for targeting of antigens to specific anatomical locations)<sup>13–18</sup>. These approaches have been used widely to study processes like peripheral tolerance induction, organ-specific autoimmunity, and anti-tumor immunity against developing tumors. Yet, despite their creativity and utility, experimental results have been impacted by inability of previous models to allow tight spatio-temporal control over antigen expression and presentation. Inducible neoantigen models theoretically could provide this control, but most of these models fail to circumvent the process of central tolerance.

Central (thymic) tolerance occurs during T cell development, and directly impacts the presence and/or functional potential of endogenous T cells in the periphery. Low-level expression and presentation of self-antigens in the thymus leads to the “pruning” of the naïve T cell repertoire by eliminating or tolerizing thymocytes with T cell receptors (TCRs) that recognize self-antigens<sup>19–22</sup>. Therefore, to allow the study of endogenous antigen-specific naïve T cell responses in peripheral organs, an inducible neoantigen experimental model must avoid expression and presentation of the cognate antigens in the thymus. This has represented an engineering challenge for experimental models relying on genetic regulation of antigen expression, since low-level, leaky expression in thymus is often sufficient to cause tolerance or to impact the residual functional capacity of the T cells that do make it through thymic selection<sup>7, 11, 12, 23, 24</sup>.

As a consequence, many studies using genetic models have resorted to the adoptive transfer of TCR transgenic (Tg) T cells (as a source of naïve antigen-specific T cells). Yet, TCR Tg T cells often do not behave like endogenous T cells and can have altered thymic development and have very high affinity for antigens<sup>25–27</sup>. As a result, they can have artificially exuberant effector T cell responses compared with polyclonal, endogenous,

antigen-specific T cells. Moreover, inducible neoantigen models can also have leaky expression outside the thymus (in uninduced tissues), which can lead to aberrant activation of naïve TCR Tg T cells upon adoptive transfer<sup>24, 27, 28</sup>.

Due to the above issues, we have a poor understanding of endogenous antigen-specific T cell responses against neoantigens under physiologic conditions, which limits our ability to therapeutically manipulate the physiological mechanisms of T cell regulation. To overcome the aforementioned technical limitations, we have engineered the iNversion INduced Joined neoAntigen (NINJA) mouse. In this model, tissue-specific expression of genetically encoded neoantigens is the result of a double genetic recombination process that is dependent on the delivery of Cre recombinase (Cre), doxycycline (D) and tamoxifen (T). This induction mechanism, based on three separate regulatory steps, ensures switch-like induction of neoantigen expression, which bypasses thymic tolerance. This model system, therefore, enables the study of endogenous neoantigen-specific T cells following *de novo* neoantigen induction, providing an important tool for immunologists across disciplines.

## Results

### Structure of NINJA with two modules.

To achieve tight regulation over neoantigen induction, we envisioned a design for the NINJA allele that contained two modules (Figure 1a, full sequence available in Supplementary Notes). The first was a “neoantigen” module (NM) that relied on DNA inversion to regulate neoantigen expression. Inversion would be regulated by Flippase recombinase (FLPo)<sup>29, 30</sup>. FLPo would be encoded into a second “regulatory” module (RM). In the RM, FLPo would be regulated at three levels, requiring Cre-mediated recombination to “poise” the RM, followed by simultaneous D/T exposure to induce FLPo expression and activity.

### Design of the spliced NM.

To generate a module encoding a neoantigen that would not have leaky expression in the OFF state, we reasoned that the DNA sequences encoding the full-length neoantigen should not exist within the genome prior to induction. Thus, we conceived of a gene in which the neoantigen-encoding DNA sequences were split across three exons, and the second exon was inverted relative to the first and third so that the gene could not transcribe/translate the full-length peptide antigens in the OFF state (Figure 1a). Induction would be triggered by the permanent inversion of the second exon, which we determined would be achieved using FLPo and “non-compatible” FRT sites<sup>29, 30</sup>.

First, we identified neoantigens that had immunological tools for their analysis (*i.e.*, MHC class I and class II tetramers, TCR Tg mice, *etc.*) and had sequences that could be engineered to contain in-frame splice donor and acceptor sites (Extended Data Figure 1a). Thus, we settled on well-characterized antigens from the glycoprotein (GP) of the lymphocytic choriomeningitis virus (LCMV), which are recognized by H2-D<sup>b</sup>-restricted CD8 T cells (GP33–43: **KAVY**NFATCGI) and H2-I-A<sup>b</sup>-restricted CD4 T cells (GP66–77: IY**KGVY**QFKSV) [splice sites were inserted between the amino acids noted in bold]. GP33–43 and GP66–77 are also recognized by T cells from P14 and SMARTA CD8 and

CD4 TCR Tg mice, respectively. *In silico*, we inserted RNA splice sites into the DNA and created two introns (Extended Data Figure 1b). We also inverted the sequences encoding exon 2, so that in the OFF state, the construct would splice directly from exons 1 to 3. To allow for induction of neoantigens in response to FLPo, we inserted non-compatible FRT sites (F3 and FRT Wt;<sup>29</sup>) to flank the inverted exon 2 sequence so that exposure to active FLPo would cause a permanent inversion of exon 2 (Extended Data Figure 1c,<sup>31</sup>).

Over the course of 7 iterative versions (NM.1-NM.7, see methods; Extended Data Figure 2a), we refined the design of the NM to ensure that the constructs had high fidelity before and after FLPo-mediated recombination (Extended Data Figures 2b–c). We modified the construct so that the inducible neoantigen was incorporated into the coding sequence of GFP in such a way that a non-fluorescent N-terminal portion of GFP was produced when the NM was OFF (before recombination) and full-length fluorescent GFP containing the neoantigens was produced when the module was ON (after recombination; Figure 1a and Extended Data Figure 3). Finally, we confirmed that the construct was unable to produce a cross-tolerizing GP33–43 peptide when the NM was in the OFF state (Extended Data Figure 4).

### Validating the final NM construct.

To test the final NM construct (NM.7) for functionality, we transfected 293T cells with the construct in the presence or absence of a plasmid encoding FLPo. After 72 hours, flow cytometric (FC) analysis of the transfected cells showed robust GFP fluorescence in 293T cells transfected with the NM and FLPo, but no detectable fluorescence when FLPo was not co-transfected (Figure 1b). This corresponded with a change in the size of the protein from 19.9 kDa to 34.3 kDa (Figure 1c). We also isolated plasmid DNA from NM/FLPo co-transfected 293T cells and confirmed that the RM had been faithfully recombined by DNA sequencing. We use this FLPo-recombined NM construct (NM.7A) below.

Next, we assessed the ability of the constructs to elicit responses by GP33-specific CD8 T cells. For this, we transiently transfected a dendritic cell line (DC2.4) with the NM.7 (NINJA OFF) or NM.7A (NINJA ON) construct. We cultured the transfected DC2.4 cells for 4 days alone or with Cell-Trace Violet (CTV)-labeled GP33-specific CD8 T cells from P14 mice. In this assay, if P14 T cells recognize GP33–43 presented by DC2.4 cells, they become activated (dilute CTV and increase CD44 expression) and kill the adherent DC2.4 cells (leading to loss of crystal violet staining). In NM.7 transduced wells, the P14 T cells remained naïve and the DC2.4 cells formed a confluent monolayer (Figures 1d–e). By contrast, when DC2.4 cells were transfected with NM.7A, P14 T cells proliferated and killed the DC2.4 cells. Together, these data demonstrate that NM.7 is non-immunogenic in the OFF state and immunogenic in the ON state.

### Design of the RM.

We designed the RM to contain a Cre-inducible FLPo that was fused to amino acids 251–596 of the human estrogen receptor (ER) (FLPoER) and was expressed under the control of the doxycycline-inducible pTRE-tight promoter (Figure 1a and Extended Data Figure 5). Similar to the NM, the DNA sequences encoding FLPoER in the RM were spliced and split into two exons that were encoded in opposite orientations. Thus the RM required Cre-

mediated inversion before it could produce a functional protein (Figure 1a). We refer to this post-Cre exposure state as the “poised” state because FLPO activity requires subsequent D/T treatment. For this to happen, cells must also express the reverse tetracycline transactivator (rtTA), potentially adding an extra layer of specificity (*i.e.*, tissue-specific promoters expressing rtTA).

### Assembly and testing of NINJA targeting construct.

We inserted the RM and NM into a *Rosa26* targeting construct such that they were oriented in opposite directions (Figure 1a and Extended Data Figure 6). This was done to avoid transcriptional interference in the RM from the endogenous *Rosa26* locus promoter. To minimize the impact of the CAG promoter (in the NM) on the pTRE promoter in the RM, we inserted the 2x chicken gamma globulin (CGG) insulator between the RM and NM. These parts completed the fully assembled NINJA targeting construct (NINJA TC).

Next, we tested the NINJA TC in 293T cells. In the absence of Cre the NM remained OFF (GFP-), even when the cells were treated with D/T. By contrast, when cells were co-transfected with NINJA TC, Cre, and rtTA, it was possible to turn the NM ON (GFP+) with D/T treatment (Figure 1f). These data confirm that NINJA TC functions as designed and induces neoantigens after cumulative Cre, D, and T treatment.

### Generating a NINJA-containing lung adenocarcinoma cell line.

To test the functionality and fidelity of the components of the RM and NM in the endogenous genomic context of the *Rosa26* locus, we used a murine *Kras*<sup>G12D</sup>, *p53*<sup>-/-</sup> (KP) lung cancer cell line to generate a knock-in monoclonal cell line containing the NINJA TC (KP-C4) (Figure 2a). We then transduced KP-C4 cells with an rtTA-encoding retrovirus (KP-C4A3) and infected them with a recombinant Cre-expressing adenoviral vector (Ad-Cre) to cause a recombination in the RM and place it *permanently* in the poised state (KP-C4A3D6) (Figure 2a). We verified that the NM in the KP-C4A3D6 cell line remained OFF for over 20 passages in culture (based on GFP fluorescence, not shown). However, when the KP-C4A3D6 cell line was infected with a recombinant adenoviral vector expressing FLPO (Ad-FLPO, positive control) or treated with D and 4-hydroxytamoxifen (4-OHT), these cells turned ON the NM and expressed GFP (Figure 2b).

To test immunogenicity, we sorted a pure GFP+ population of neoantigen expressing (ON) KP-C4A3D6 cells and compared these cells *in vivo* versus KP-C4A3D6 that had never been exposed to D/T (OFF, Figure 2b). We implanted the ON and OFF cells intramuscularly (I.M.) in opposite legs of C57BL/6 (B6) mice along with adoptively transferred GP33-specific firefly-luciferase (fLuc)-expressing P14 T cells. This allowed us to track the accumulation of neoantigen-specific CD8 T cells in the tumors by *in vivo* bioluminescence imaging (IVIS). After 11 days, we observed accumulation of fLuc+ P14 T cells in the neoantigen-expressing ON tumors, but not in the neoantigen-negative OFF tumors (Figure 2c). FC analysis confirmed infiltration of neoantigen-specific CD8 T cells into neoantigen-expressing tumors, consistent with local cognate antigen exposure (Figures 2d–e). Tumor growth rates for antigen ON tumors, but not antigen OFF tumors, were decreased in a T-cell-dependent manner (Figure 2f).

One of the unique advantages of the NINJA system is the ability to induce the expression of neoantigens in established tumors *in vivo*. To test this, mice with fLuc<sup>+</sup> P14 T cells were implanted with KP-C4A3D6 cells (I.M.) and were subsequently treated with D/T beginning six days post-transplant. T cell responses were only observed in D/T treated mice or ON controls, with responses visible one day after D/T treatment (Figure 2g). Together, these data confirmed that NINJA is a tightly regulated, switch-like induction system that is activated by D/T administration *in vitro* and *in vivo*.

### **NINJA mice are not tolerant to their neoantigens.**

Having successfully generated and tested the NINJA TC, we next generated *Rosa26* knock-in NINJA mice on a B6 genetic background (Extended Data Figure 7). NINJA mice were born at the expected mendelian frequencies and had no distinguishing phenotypes compared to wild-type B6 mice. These mice were then crossed to generate NINJA x CAG-rTA3 mice (referred to as NINJA, unless otherwise stated). We first assessed whether there was baseline leaky expression of neoantigens in NINJA mice by looking at the frequency of GFP<sup>+</sup> cells in their peripheral blood mononuclear cells (PBMCs; Figure 3a). As positive controls, we bred NINJA mice to FLPo Tg mice to generate lines that had germline recombination of the NM and therefore ubiquitous constitutive expression of neoantigens (NINJA-F). We also generated NINJA x Cre Tg (NINJA-C) mice, where the RM is in the poised state in all cells. In NINJA-F mice, all PBMCs were GFP<sup>+</sup>, while no PBMCs were GFP<sup>+</sup> in NINJA mice, suggesting that there is no leaky neoantigen expression. Interestingly, in NINJA-C mice, >99% of PBMCs remained GFP<sup>-</sup>, although we were able to detect a very small fraction of GFP<sup>+</sup> cells (<1%) (Figure 3a; note, this fraction increases with age). These data suggest that the NINJA allele in mice remains very tightly regulated, except under extreme circumstances where regulatory elements are compromised at the germline level.

To test for central tolerance towards GP33–43 and GP66–77, we bred NINJA mice to P14 or SMARTA mice, and analyzed developing thymocytes. Development of CD8 and CD4 T cells in P14 x NINJA and SMARTA x NINJA mice, respectively, was comparable to parental P14 or SMARTA strains (Figure 3b and Extended Data Figure 10). By contrast, severe defects in T cell development were evident in P14 and SMARTA x NINJA-F and P14 and SMARTA x NINJA-C mice (Figure 3b and Extended Data Figure 10).

Consistent with their lack of central tolerance, NINJA mice had robust GP33-specific CD8 and GP66-specific CD4 T cell responses to acute LCMV infection, which were indistinguishable from the responses of T cells in control B6 mice. By contrast, NINJA-F and NINJA-C mice were completely tolerant to GP33 and GP66, but did respond to NP396 (a non-cross reactive antigen from LCMV, Figures 3c–d). Finally, to confirm that the environment of NINJA mice did not induce peripheral tolerance, we “parked” adoptively transferred P14 CD8 T cells in B6, NINJA, NINJA-F, or NINJA-C mice for 14 days and then infected them with LCMV Armstrong. The transferred P14 CD8 T cells could still provide robust responses to LCMV after 14 days of exposure to the B6 or NINJA environment, but responses were >800-fold and >35-fold reduced after exposure to the environments of the NINJA-F and NINJA-C mice, respectively (Figure 3e). This finding is consistent with a

process of peripheral tolerance induction in NINJA-C and NINJA-F mice, but not NINJA mice.

### Activation of the NM leads to presentation of neoantigens *in vivo*.

To test the functionality of the NM, we generated bone-marrow-derived dendritic cells (BMDCs) from NINJA mice and infected them with either a recombinant GFP-expressing adenoviral vector (Ad-GFP, control) or Ad-FLPo. We then used these BMDCs to immunize B6 recipients that had previously received  $2.5 \times 10^4$  Thy1.1/1.1+ P14 T cells and  $2.5 \times 10^4$  Thy1.1/1.2+ SMARTA T cells. The P14 T cells and the SMARTA T cells responded to the immunization by expanding, and were only detectable in the mice that received Ad-FLPo-treated NINJA BMDCs (Figure 4a, bottom) and not Ad-GFP-treated NINJA BMDCs (Figure 4a, top).

To test *in vivo* induction of neoantigens in NINJA mice, we adoptively transferred fLuc+ P14 T cells into NINJA mice and infected them with  $10^7$  PFU of Ad-FLPo in the footpad (subcutaneous, S.C.), muscle (I.M.), liver (intravenous, I.V.), or lungs (intratracheal, I.T.). In all cases, we observed accumulation of fLuc+ P14 T cells specifically at the infected site by IVIS imaging (Figure 4b). Moreover, this system allowed us to track the kinetics and location of neoantigen-specific T cells after neoantigen induction. Following S.C. infection with Ad-FLPo, P14 T cells were first located in the tissue-draining lymph nodes (dLNs), and then these cells migrated to the sites of neoantigen expression (Extended Data Figure 8). This suggests that neoantigens were expressed in the treated tissue shortly after infection and functionally presented in local draining organs, leading to activation of neoantigen-specific T cells.

To determine if the neoantigen-specific T cells were directly interacting with neoantigen-expressing cells, we performed the same experiment as above, but used dsRed-expressing P14 T cells. Eight days after infection, we observed dsRed+ P14 T cells localized in the infected footpad in direct proximity to GFP+ skin cells (Figure 4c). We also observed signs of immunopathology in the infected tissue, including the infiltration of CD3+ cells and thickening of the epidermal and dermal layers of the skin (compared to non-infected footpad, Figures 4d–e). Together, these data show that neoantigens in NINJA are inducible and recognized by neoantigen-specific T cells *in vivo*.

### Endogenous T cell responses to neoantigen induction *in vivo*.

To determine whether *in vivo* induction of the NM could trigger endogenous neoantigen-specific CD8 T cell responses, we infected NINJA mice in the footpad with  $10^7$  PFU Ad-FLPo and analyzed the dLNs 8 days later. We observed robust self-neoantigen-specific responses from endogenous GP33-specific CD8 T cells (Figure 5a). Moreover, the T cells were polyfunctional, as indicated by their expression of Granzyme B and of their capacity to produce the pro-inflammatory cytokines IFN $\gamma$  and TNF $\alpha$  (Figure 5b). Signs of an anti-self-tissue response with consequent immunopathology were also detected in the infected footpad following local administration of Ad-FLPo (Figure 5c). Finally, we observed that GP33-specific T cells persisted long-term in the dLNs after *in vivo* neoantigen induction with S.C. Ad-FLPo (day 35) (Figure 5d), thus suggesting the development of neoantigen-

specific memory T cells in NINJA. These data confirm that *in vivo* activation of the NINJA NM in the context of adenoviral infection results in strong endogenous neoantigen-specific T cell responses.

### Induction of neoantigens mediated by RM *in vivo*.

Next, we tested whether the RM was functional *in vivo* by infecting NINJA mice in the footpad with  $10^7$  PFU Ad-Cre and treating them with D/T or vehicle control at the time of infection (day 0). Critically, robust endogenous GP33-specific CD8 T cell responses were observed 8 days after infection, but only when mice were also treated with D/T (Figure 6a). Moreover, we also tested whether it was possible for us to uncouple Cre delivery/expression from neoantigen induction by waiting 14 days before treating Ad-Cre infected NINJA mice with D/T. Similar to day 0 D/T treated mice, we observed robust T cell responses 8 days after the later administration of D/T (Figure 6a).

The above data suggested that the poised regulatory module was not leaky in the context of adenoviral infection. However, it remained possible that there was an endogenous GP33-specific CD8 T cell response at levels below the limit of detection. To address this, we infected NINJA mice in the footpad with 1:9 mixtures of Ad-FLPo:Ad-GFP or Ad-FLPo:Ad-Cre. In this context, because Ad-FLPo:Ad-GFP elicits a detectable GP33-specific CD8 T cell response (Extended Data Figure 9), we could determine whether Ad-FLPo:Ad-Cre enhanced this response due to leaky neoantigen expression. Critically, the response to Ad-FLPo:Ad-Cre was quantitatively similar to the response elicited by Ad-FLPo:Ad-GFP (Extended Data Figure 9), suggesting that the poised state of the RM allows for tight regulation over neoantigen induction after Ad-Cre delivery. Together, these data demonstrate that the RM can be used to achieve tight spatio-temporal control over neoantigen expression and endogenous T cell responses, even allowing for the separation of Cre exposure and neoantigen induction.

### Inducible expression of neoantigens in NINJA mice using endogenous genetic elements.

We next tested whether NINJA could be used to achieve localized neoantigen expression and neoantigen-specific T cell responses without exogenous delivery of Cre. For this, we crossed NINJA mice to *Rosa26-CreER* mice. Unlike NINJA-C mice, NINJA x CreER (NINJA-C-ER) mice had a robust capacity to mount GP33-specific responses following acute infection with LCMV that was on par with NINJA mice (Figure 6b). Systemic administration of D and topical administration of T resulted in localized responses to neoantigens by fLuc<sup>+</sup> P14 T cells in the T-treated areas of the skin (red box in Figure 6c). Moreover, this treatment strategy also elicited endogenous GP33-specific T cell responses (Figure 6d). Taken together, these data indicate that the RM of NINJA mice can be used to induce localized expression of neoantigens in a given tissue and to study responses by endogenous neoantigen-specific T cells without the need for exogenous Cre delivery.

## Discussion

One of the barriers in studies of T cell immunology has been the absence of mouse models that allow spatio-temporal regulation of antigen expression while also preventing

development of central tolerance towards the inducible neoantigen<sup>7, 8, 11, 12, 23, 24</sup>. Here we described the NINJA model, which bypasses central tolerance by creating a neoantigen *de novo* in a peripheral tissue. We demonstrated that tight regulation through the RM enabled “switch-like” induction of expression from the NM without leakiness. Thus, the presence of the OFF state NINJA allele did not impact the development of the endogenous T cell repertoire. Moreover, we demonstrated that once induced, NINJA was capable of eliciting T cell responses in the context of a transplantable tumor model, infection with recombinant adenoviral vectors expressing FLPo or Cre, and a transgene expressing CreER. Furthermore, neoantigen induction and endogenous antigen-specific T cell responses were dependent on the administration of D/T. Together, these data demonstrate that NINJA offers tight spatio-temporal regulation of inducible neoantigen expression *in vivo* and is capable of eliciting physiologic responses by endogenous T cells.

The high sensitivity of developing thymocytes to low-level expression of self-antigens on medullary thymic epithelial cells (mTECs) is critical for eliminating potential self-reactive T cells and preventing autoimmunity<sup>19, 20</sup>. However, leaky thymic expression has confounded previous attempts to develop mouse models for inducible neoantigens. NINJA uses multiple levels of regulation to avoid leaky expression, but, as demonstrated by NINJA-C mice, the removal of just one of these regulatory layers led to complete central tolerance. Moreover, despite the fact that <1% of cells express the neoantigens, tolerance in NINJA-C mice is on par with that observed in NINJA-F mice where all cells express the neoantigens (Figure 3). In previous inducible neoantigen models it was conceivable that low-level leaky expression from many cells in the thymus led to central tolerance<sup>7, 11, 12, 24</sup>. NINJA-C mice have a different pattern of leaky neoantigen expression characterized by a handful of cells with high neoantigen expression levels. In this way, NINJA-C mice may more closely reflect the natural biology of central tolerance, as only a small fraction of mTECs (<5%) efficiently express a given tissue-restricted self-antigen<sup>21</sup>. Further work will be required to determine whether lower levels of antigen expression under these conditions could facilitate other outcomes from thymic selection, for example T cells escaping into the periphery with some residual functions intact, as was described previously<sup>11, 24</sup>. NINJA might also allow for an inducible model for exploring central tolerance mechanisms *in vivo*.

The LCMV-derived peptides GP33–43 and GP66–77 were chosen as neoantigens in NINJA because many tools have been developed for studying T cell biology using these peptides. However, the NINJA allele also has other potential neoepitopes, including two previously described epitopes (Kb-GP34–41 and Db-GP67–77). Critically, these epitopes vary in strength from the Db-GP-33–43 neoantigen that we focused on, with stronger and weaker binding affinity for MHC class I, respectively (Supplementary Table 1,<sup>32</sup>). Cre and rtTA3 also contain potential neoantigens, but their immunogenicity in experimental settings will largely depend on the method of delivery. FLPoER251 contains several potential neoantigens, but the protein itself is only expressed when NINJA mice are fed doxycycline. Thus, these neoantigens are transient in the cells and may not have a significant impact on T cell responses. In line with this, T cell depletion did not increase the growth of KP-C4A3D6 OFF cells even though they contained the poised RM (Figure 2f). Maintaining mice on doxycycline could be a means for increasing neoantigen diversity under experimental protocols where that is desired. Similarly, responses to additional inducible neoantigens can

be studied by crossing NINJA mice to mice with different MHC haplotypes. For example, while the stronger neoantigens are in the N-terminal portion of GFP in the H-2b background, on the H-2d background, the C-terminal portion of GFP contains a well-characterized strong neoantigen (Kd-GFP200–208) that is recognized with high affinity by the T cells from JEDI TCR transgenic mice<sup>28</sup>. Thus, NINJA offers considerable flexibility to address experimental questions relating to neoantigen number and strength.

The tight spatio-temporal control over neoantigen expression gives NINJA the potential to be used as a model in a variety of experimental settings where the study of endogenous T cells in peripheral organs is desired. For example, with NINJA, the same model antigens can be expressed in a selected tissue under either inflammatory conditions or in the absence of overt inflammation. We demonstrated that the former can be achieved by delivery of FLPo or Cre with a viral vector (Figures 4–5), while the latter can be achieved by crossing NINJA mice with mice carrying a Cre transgene and treating with D/T (Figure 6). These experimental settings would allow the use of NINJA to investigate how different tissue environments and/or different pro-inflammatory cues impact neoantigen-specific T cell functions. Moreover, these approaches will be useful for studying the mechanisms of peripheral tolerance induction. Here, it is worth noting that crossing NINJA mice to some Cre transgenic mice leads to tolerance prior to neoantigen induction. In our experience, we have found that central tolerance is dependent on the promoter of the transgene. Furthermore, we have found that CreER transgenes do not lead to central tolerance in the absence of D/T (Figures 3 and 6), suggesting that an additional layer of regulation on Cre activity may be necessary to avoid tolerance before induction.

Importantly, we have designed the NINJA system to be compatible with most Cre-dependent genetically engineered cancer models, so that one can achieve tumor-specific expression of neoantigens. When crossed to such models, a unique feature of NINJA is the ability to uncouple tumor initiation (driven by Cre) from neoantigen expression by tumor cells (driven by D/T). As genetic mutations/neoantigens can be accumulated by tumors over time, we anticipate that this will be a useful feature for experiments that aim to mimic the natural evolution of tumors and the concurrent anti-tumor immune response.

Lastly, the mechanisms that lead to autoimmunity are poorly understood. Depending on the type of autoimmune disease, the ability of self-reactive T cells to escape central tolerance may be critical for enabling the T cell autoimmune response. For example, some T cell clones causing type I diabetes in NOD mice and humans are likely to recognize insulin epitopes created by post-translational modifications that occur in pancreatic beta cells but not in the thymus<sup>33–35</sup>. This scenario is not unique to diabetes, as similar phenomena have also been described in a number of other autoimmune conditions<sup>36–39</sup>. NINJA is able to recapitulate this key feature by circumventing central tolerance, and allowing experimental control over where neoantigens will ultimately be expressed. Therefore, when crossed onto autoimmune-prone backgrounds, NINJA should allow for the study of self-antigen specific T cell responses in different tissues, and potentially a better understanding of many autoimmune processes.

## Online Methods

All studies were carried out in accordance with procedures approved by the Institutional Animal Care and Use Committees of Yale University and the Massachusetts Institute of Technology. All mice were bred in specific pathogen-free conditions. For experiments, 6–12 week old mice were used. The Life Sciences Reporting Summary is available with online methods.

Development and testing of NM and RM constructs and full DNA sequence detailed in Supplementary Notes.

### Assembly of the NINJA targeting construct:

The RM and NM were inserted into the pzDonor Rosa26 targeting construct separated by the 2xCGG insulator to minimize the impact of the CMV enhancer on the pTRE-tight promoter. Moreover, a pgk-puromycin resistance cassette was inserted into the RM in such a way that the HSV poly A sequence was predicted to terminate transcription downstream of the Rosa26 promoter. However, the puromycin resistance cassette is lost following Cre-mediated recombination, providing an assay for recombination at this allele.

### Transient transfection of 293T cells for DNA isolation, *in vitro* induction of NINJA, Western Blot and IF

293T cells were cultured in complete DMEM (ThermoFisher Scientific cat. 11965118 +10% HI-FBS, 1x Pen/Strep) and then transfected using the LipoD293 Transfection reagent (SigmaGen Laboratories, cat. SL100668) according to manufacturer's instructions.

For DNA isolation, cells were transfected and harvested 48hr later and digested at 55°C overnight in lysis buffer (0.2 M Tris HCl, 0.15M NaCl, 2mM EDTA, 1% SDS, 50 µg/mL Proteinase K in nuclease-free H<sub>2</sub>O), then quenched with saturated NaCl. DNA was precipitated by incubation of supernatant with cold 100% EtOH, washed in cold 70% EtOH, dried and resuspended in nuclease-free H<sub>2</sub>O.

For *in vitro* induction of NINJA, 293T cells were transfected with 1 µg NM.7 construct + 0.3 µg of Cre, Cre/rtTA, rtTA, or FlpO construct. 24 hours later, 1 µg/mL of doxycycline (Millipore Sigma, cat. D9891) and 1 µg/mL of 4-OHT (Millipore Sigma, cat. SML1666) were added to the culture media. After 72 hours doxycycline was removed and cells were cultured in regular media for 24 more hours prior to harvesting. Before flow, cells were washed 3x in PBS + 2% FBS to reduce autofluorescence from doxycycline carryover. GFP expression was measured by flow cytometry on a BD Accuri C6 analyser or BD LSRII analyser (BD Biosciences).

For Western Blot, 293T cells were transfected with 0.5 µg/mL target construct + 0.15 µg/mL FlpO construct. Total proteins were harvested after 72 hours using RIPA lysis reagent protocol (ThermoFisher Scientific, cat. 89900). Protein content was quantified by BCA assay (ThermoFisher Scientific, cat. 23225), and 3–5 µg total protein were mixed in 1x LDS Sample Buffer + 1x sample reducing reagent, loaded on BOLT or NuPage 4–12% BisTris precast gel (ThermoFisher Scientific, cat. NW04122BOX) and run with SeeBlue2

Protein Ladder (ThermoFisher Scientific, cat. LC5925). Western Blotting was performed according to Invitrogen's MiniBlot Western System procedures. Briefly, anti-GFP (N-terminus) (clone D5.1, Cell Signaling Technology) or anti-Grp94 (loading control) (Cell Signaling Technology, cat. 2104) primary antibodies were left overnight at 4C in 10% Milk in TBS-T (Tris-HCl, Tris Base, NaCl, distilled water, 0.1% Tween 20). HRP-conjugated goat anti-rabbit secondary antibody (ThermoFisher Scientific, cat. 656120) was incubated for 1 hour at room temperature. Blot was imaged using Pierce ECL (ThermoFisher Scientific, cat. 32106) or Pierce SuperSignal West Femto ECL kits (ThermoFisher Scientific, cat. 34096).

For IF, 293T cells were transfected with 1.5 µg of the indicated construct (NM.5 or NM.7 with neoantigen either ON or OFF) and 72hr later were fixed in 2% PFA for 20 minutes. Staining was performed as described<sup>47</sup> using a primary antibody specific for a linear epitope of the N-term portion of GFP (clone D5.1, Cell Signaling Technology) or for a conformational epitope of GFP to detect correctly folded GFP (clone 3E6, Invitrogen).

### Lymphocyte isolation from spleen and LNs

Organs were processed as described<sup>5</sup>. To purify CD8 T cells from the spleen of TCR Tg P14 mice, the EasySep Kit (StemCell Technologies, cat. 18000 and cat. 19853) was used according to manufacturer's instructions.

### DC2.4 proliferation and killing assay

DC2.4 cells were transfected with 1 µg of target construct using the Lipofectamine3000 transfection kit (Invitrogen, cat. L3000008) following manufacturer's instructions. 24 hrs later, transfected DC2.4 cells were cocultured for 5 days with  $2 \times 10^6$  Thy1.1<sup>+</sup>/1.1<sup>+</sup> P14 T cells purified as detailed above and stained with Cell-Trace Violet Proliferation kit (Invitrogen, cat. C34557) according to manufacturer's instructions. Killing of DC2.4 was then assessed by Crystal Violet staining (0.1% Crystal Violet solution), while P14 T cells were stained with antibodies specific for Thy1.1 (clone OX-7, BioLegend), CD8 (clone 53-6.7, BioLegend), CD44 (clone IM7, BioLegend) and Vα2 (clone B20.1, BD Biosciences) and analysed by flow cytometry on a BD Biosciences LSRII analyser.

### KP-C4A3D6 cell transplant and in vivo P14 T cell activation

fLuc<sup>+</sup> P14 T cells were harvested from fLuc<sup>+</sup> P14 TCR Tg mice as detailed above, and adoptively transferred I.V. retro-orbitally into wild-type B6 recipients ( $5 \times 10^6$  fLuc<sup>+</sup> P14 T cells/mouse) one day prior to tumor transplant.  $2.5 \times 10^4$  -  $2 \times 10^5$  sorted GFP<sup>+</sup> NINJA-expressing KP-C4A3D6 cells (ON) or parental NINJA-negative KP-C4A3D6 (OFF) cells were transplanted into the leg muscle following baseline leg diameter measurement.

Tumor size was measured throughout the experimental time with a digital caliper (Thomas Scientific, cat. 1235C55) on two axes (diameter of coronal and sagittal plane of injected leg). Baseline measurements were taken prior to transplant, after shaving, and tumor sizes were adjusted for original leg volume. Volume was calculated as (coronal diameter mm)x(sagittal diameter mm)x(average of both measurements)= mm<sup>3</sup>.

At the end of the experimental time, tumors were harvested and dissociated in Collagenase IV (Worthington Biochemical, cat. LS004189) Buffer (1x HEPES buffer, 0.5 mg/mL Collagenase IV, 20 µg/mL DNase in 1x HBSS with MgCl<sub>2</sub> and CaCl<sub>2</sub>) running the default Lung\_01 protocol on a gentleMACS Dissociator instrument (Miltenyi Biotec). Tumor samples were then incubated at 37°C for 40 min (rotating) prior to running the default Lung\_02 protocol on the Dissociator. Digestion was quenched by adding 500 µl FBS. Tumor samples were then strained through 70 µm cell strainers, washed with 1% HI-FBS RPMI-1640 (ThermoFisher Scientific cat. 11875085) and red blood cells were lysed using 1x RBC Lysis Buffer (eBioscience, cat. 00–4333–57)

### BMDC Transplant

Thy1.1<sup>+</sup>/1.2<sup>+</sup> P14 T cells and Thy1.1<sup>+</sup>/1.1<sup>+</sup> SMARTA T cells were isolated from TCR Tg mice as detailed above. 10<sup>5</sup> P14 T cells and 10<sup>5</sup> SMARTA T cells were co-transferred I.V. by retro-orbital injection into wild-type B6 recipients 0–19 days prior to BMDC transplant.

BMDCs were prepared from the bone marrow of NINJA mice as described in<sup>47</sup>. Four days after bone marrow harvest, maturing BMDCs were transduced *in vitro* with 10<sup>10</sup> PFU/mL of recombinant Ad5CMVFLPo (Iowa Vector Core, VVC-U of Iowa-530HT) or 3.5 × 10<sup>8</sup> PFU/mL of recombinant Ad5CMVeGFP (Iowa Vector Core, VVC-U of Iowa-4). BMDCs were harvested 3 days later and stained with antibodies specific for CD11c (clone N418, BioLegend) and MHC-I (H-2Kb, clone AF6–88.5.5.3, eBioscience) and analysed by flow cytometry on a BD LSRII analyser (BD Biosciences). 10<sup>4</sup> CD11c<sup>+</sup>MHC-I<sup>+</sup>GFP<sup>+</sup> BMDCs were then transplanted into the footpad of B6 hosts in 15 µl PBS.

Recipient animals were euthanized 7 days after BMDC transplant to collect spleen and the draining LN (popliteal). Organs were processed as described in<sup>5</sup> and samples were stained with antibodies specific for Thy1.1 (clone OX-7, BioLegend), Thy1.2 (clone 30-H12, BioLegend), CD4 (clone GK1.5, BioLegend) and CD8 (clone 53–6.7, BioLegend). Cells were then analysed on a BD LSRII flow cytometer (BD Biosciences).

### Creation of the NINJA transgenic lung tumor cell line.

A B6 cell line derived from an Ad-CRE-infected Kras<sup>G12D</sup>, p53<sup>fl/fl</sup> mouse<sup>48,49</sup> was co-transfected with the NINJA targeting construct and RNA encoding a zinc-finger nuclease targeting the *Rosa26 locus* (Millipore Sigma) using Amaxa nucleofector (Lonza). We generated a KP-NINJA line and verified that the NINJA construct was targeted to the *Rosa26 locus*. Single-cell clones were selected based on Puro resistance and screened for incorporation of the NINJA targeting vector by PCR. The C4 clone was selected for further study. Proper targeting of the NINJA construct to the Rosa26 locus was verified by PCR. rtTA was stably introduced into C4 cells via a dual promoter retrovirus expressing rtTA and a blasticidin resistance cassette (C4A3). A blasticidin-resistant single cell clone (C4A3D6) was selected and infected with Ad-CRE to mediate recombination of the RM. Activation of the NM was achieved by incubating C4A3D6 cells *in vitro* with doxycycline (1 µg/mL) and 4-hydroxytamoxifen (1 µg/mL) for 72 hrs.

## Generation of the NINJA mouse

Targeting was performed by the Swanson Biotechnology Center Preclinical Modeling facility of MIT. Briefly, NINJA mice were generated by transfecting the PvuI-HF linearized NINJA targeting construct into B6 ES cells (JM8) along with mRNA encoding ZFNs for the *Rosa26* locus (Millipore Sigma). We screened clones for proper targeting by southern blotting and identified one correctly targeted clone (Extended Data Figure 7). We injected these targeted ES cells into B6 blastocysts and selected a high percentage chimera (>80%) for breeding to a B6 female. This breeding resulted in germline transmission in two pups that were used to produce the NINJA mouse line.

For experiments, NINJA mice were crossed to CAG-rtTA3 transgenic mice (JAX, stock # 016532), unless otherwise noted.

NINJA-F and NINJA-C mice were generated by crossing NINJA mice that did not carry the CAG-rtTA3 transgene to FLPe or Cre deleter mice (JAX, stock # 003946) and (JAX, stock # 006054) respectively and then crossing FLPe+ or Cre+ F1 mice to B6 mice and screening the progeny for FLPe- or Cre-driven recombination at the NINJA locus. Mice were bred to homozygosity and maintained as independent strains.

NINJA mice will be deposited in Mutant Mouse Resource & Research Centers at Jackson laboratories (strain 66733, B6J.B6N-Gt(ROSA)26Sortm1(tetO-flpo\*/ERT2,CAG-GFP\*)Nijo; NINJA Mice)

## Genotyping of NINJA, NINJA-C, and NINJA-F mice

NINJA mouse tail DNA was amplified using KAPA Taq PCR Kit (Takara Bio, cat. R040A) and primers Rosa26 WT F, Rosa26 WT R, and Rosa26 Ninja R (Supplementary Table 2). Expected bands were 378 bp for WT allele and 280 bp for NINJA allele. For NINJA-C, Rosa26 WT F, Rosa26 NINJA R, and Rosa26 Ninja-C R primers were used for expected bands of 280 bp for unrecombined NINJA allele or 694 bp for NINJA allele with recombination in RM. For NINJA-F mice, Rosa26 Ninja-F F and Rosa26 Ninja-F R primers were used for expected bands of 784 bp for unrecombined NINJA or 442 bp for NINJA allele with recombination in RM.

## Southern Blot

DNA from ES cell clones was digested with BamHI or EcoRV overnight and then was run on a 0.7% TAE gel overnight at 25–35 V. Gel was HCl depurinated, NaOH denatured, and neutralized using standard protocols and transferred passively to Hybond XL membrane via wicking method. Blot was UV-crosslinked using a Stratalinker (Stratagene) and was probed using dCTP-32P labeled probes made using the PrimeIT II kit (Agilent, cat. 300385) and Roche Quick Spin Columns (TE, cat. 11532015001). The template for the southern probe was made from a 817 bp fragment amplified from B6 genomic DNA with primers Rosa26 southern probe F and R (Supplementary Table 2,<sup>50</sup>).

### **P14/SMARTA crosses**

NINJA, NINJA-C and NINJA-F mice were crossed with either GP33-specific TCR Tg P14 mice or with GP66-specific TCR Tg SMARTA mice. Developing T cells were harvested from the thymus of 6–8 week old litters and analysed by flow cytometry on a BD Biosciences LSRII analyser after staining with antibodies specific for Thy1.2 (clone 30-H12, BioLegend), Thy1.1 (clone OX-7, BioLegend), CD8 (clone 53–6.7, BioLegend), CD4 (clone GK1.5, BioLegend).

### **Analysis of PBMCs for NINJA expression**

6–10 week old NINJA, NINJA-C, NINJA-F and wild-type B6 mice were bled retro-orbitally using heparinized glass capillaries (Fisher Scientific, cat. 22362566) to collect 50–100  $\mu$ l of blood into 0.04% Citrate Buffer. Red blood cells were lysed using 1x RBC Lysis Buffer (eBioscience, cat. 00–4333–57) and the remaining PBMCs were analysed by flow cytometry on a BD Biosciences LSRII analyser for detection of GFP expression.

### **LCMV-Armstrong infections**

7–10 week old NINJA, NINJA-F, NINJA-C, NINJA-C-ER or age-matched wild-type B6 mice were infected intraperitoneally with  $2 \times 10^5$  PFU/mouse of LCMV-Armstrong. For P14 T cell tolerance induction assay, Thy1.1<sup>+</sup>/1.1<sup>+</sup>  $10^6$  P14 T cells were adoptively transferred through retro-orbital I.V. injection into recipient mice two weeks before infection with LCMV-Armstrong. Mice were euthanized 8 days after infection to collect and process spleens as described<sup>5</sup>.

### **In vitro antigen-specific restimulation and flow cytometry**

For antigen-specific restimulation,  $1 \times 10^6$  splenocytes were cultured for 6 hrs at 37°C in 5% CO<sub>2</sub> in complete RPMI-1640 (10% HI-FBS, 55  $\mu$ M beta-mercaptoethanol, 1x Pen/Strep and 1x L-Glut) supplemented with LCMV GP33–41 peptide KAVYNFATM (0.5  $\mu$ g/mL, AnaSpec, cat. AS-61296) or left unstimulated.

For flow cytometric analysis,  $1 \times 10^6$  splenocytes or LN cells were stained with antibodies specific for surface markers Thy1.2 (clone 30-H12, BioLegend), Thy1.1 (clone OX-7, BioLegend), CD8 (clone 53–6.7, BioLegend), CD4 (clone GK1.5, BioLegend), CD44 (clone IM7, BioLegend) and tetramers for either H2Db/GP<sub>33–43</sub>-specific CD8 T cells, H2Db/NP<sub>396–404</sub>-specific CD8 T cells or I-A<sup>b</sup>/GP<sub>66–77</sub>-specific CD4 T cells (all from NIH Tetramer Core Facility). For intracellular staining, cells were processed using the Fixation/Permeabilization kit from BD Biosciences (BD Cytfix/Cytoperm, cat. 554714) following manufacturer's instructions and stained with antibodies specific for IFN $\gamma$  (clone XMG1.2, BD Biosciences) and TNF $\alpha$  (clone MP6-XT22, eBioscience). Samples were analysed on a BD Biosciences LSRII flow cytometer. Analysis of frequency and mean fluorescence intensity (MFI) was performed using FlowJo software. MFI was defined as the geometric mean of the fluorescence signal of interest for a given gated population.

### Adenoviral vector infections and *in vivo* induction of NINJA

7–10 week old NINJA mice or age-matched wild-type B6 mice were infected with a dose of  $10^7$  PFU/mouse of recombinant Ad5CMVFLPo (Iowa Vector Core, VVC-U of Iowa-530HT), Ad5CMVCre (Iowa Vector Core, VVC-U of Iowa-5-HT) or Ad5CMVeGFP (Iowa Vector Core, VVC-U of Iowa-5-HT). Adeno vectors were either injected retro-orbitally (I.V.), intratracheally (I.T.), intramuscularly (I.M.) or subcutaneously in the footpad (S.C.), depending on the experiment.

For induction of neoantigen with Ad5CMVCre infection, mice were fed doxycycline-containing food (Envigo Teklad, cat. TD.120769) for four consecutive days starting one day prior to S.C. infection with Ad5CMVCre. Mice also received two consecutive doses of a 50 mg/mL solution of 4-hydroxytamoxifen (Millipore Sigma, cat. T176) in DMSO (AmericanBIO, cat. AB03091) that was painted on the surface of the infected footpad (10–20  $\mu$ l/footpad) immediately following infection with Ad5CMVCre and the day after infection.

### Genetic induction of neoantigen expression in NINJA-C-ER mice

NINJA-C-ER mice were fed doxycycline-containing food (Envigo Teklad, cat. TD.120769) for ten consecutive days and received four doses of a 50 mg/mL solution of 4-hydroxytamoxifen (Millipore Sigma, cat. T176) in DMSO (AmericanBIO, cat. AB03091) that was painted on a selected area of the skin on the back every other day starting one day after adding doxycycline food (10–20  $\mu$ ls/mouse/dose). Endogenous T cell responses to the neoantigens were analysed by euthanizing mice 6 days after completing induction with D/T to collect the LNs draining the T-treated site. LN cells were processed and analysed by flow cytometry as indicated above.

### *In vivo* imaging by IVIS

For *in vivo* imaging of mice implanted with tumor cells, equal numbers (from  $2.5 \times 10^5$  -  $2 \times 10^6$ ) GFP<sup>+</sup> and GFP<sup>-</sup> KP-NINJA (KP-C4A3D6) cells were implanted intramuscularly (I.M.) in opposite legs of shaved B6 mice (1 to 14 days before), and adoptively transferred with  $10^4$  fLuc<sup>+</sup> P14 T cells by retro-orbital injection (I.V.). Mice were imaged on IVIS as detailed below on days 2, 7, 9, and 11 or 12 after tumor transplant. Tumors were measured every other day as detailed above.

For *in vivo* imaging of mice following adenoviral vector infection, mice were adoptively transferred with  $5 \times 10^3$  fLuc<sup>+</sup> P14 T cells by retro-orbital injection (I.V.) one day prior to infection with Ad5CMVFLPo. IVIS was performed 8 days after infection.

For *in vivo* imaging of NINJA-C-ER mice after genetic neoantigen induction,  $10^6$  fLuc<sup>+</sup> P14 T cells were transferred by retro-orbital injection (I.V.) one day prior to starting neoantigen induction with D/T. IVIS was performed 1 day after completing D/T regimen.

For imaging, hair was removed and mice were injected I.V. with a PBS solution containing 3 mgs of luciferin/mouse (XenoLight D-Luciferin - K+ Salt, PerkinElmer, cat. 122799) and imaged using an IVIS Spectrum *In Vivo* Imaging system (PerkinElmer) instrument.

## IF/IHC

For IF/IHC, mice were adoptively transferred with  $5 \times 10^3$  dsRED<sup>+</sup> P14 T cells by retro-orbital injection (I.V.) one day prior to S.C. infection with Ad5CMVFLPo in the footpad. 8 days after infection, mice were euthanized to collect infected footpads and the untreated contralateral footpads (negative control). For IF, tissues were fixed overnight at 4°C with a paraformaldehyde-lysine-periodate fixative (PLP), subsequently cryoprotected with 30% sucrose in PBS for 6–8 hrs at 4°C, and then embedded in cryomolds with 100% optimum cutting temperature (O.C.T.) compound (VWR, cat. 25608–930) on dry ice for freezing.

For IHC, tissues were fixed in a 1x formaldehyde solution in PBS (Millipore-Sigma) and then embedded in paraffin and sectioned by the Yale Pathology Core Facility. All tissues were sectioned and stained as described previously<sup>47</sup>. Image analysis was performed using Leica LAS-X (IF) or NIS-Elements (Nikon) (IHC) softwares.

## Neoantigen Binding Predictions

The predicted binding strengths of epitopes in Table S1 were obtained using the NetMHC-4.0 method for the prediction of peptide-MHC class I binding affinity using gapped sequence alignment, publicly available at: <http://www.cbs.dtu.dk/services/NetMHC-4.0><sup>51, 52</sup>.

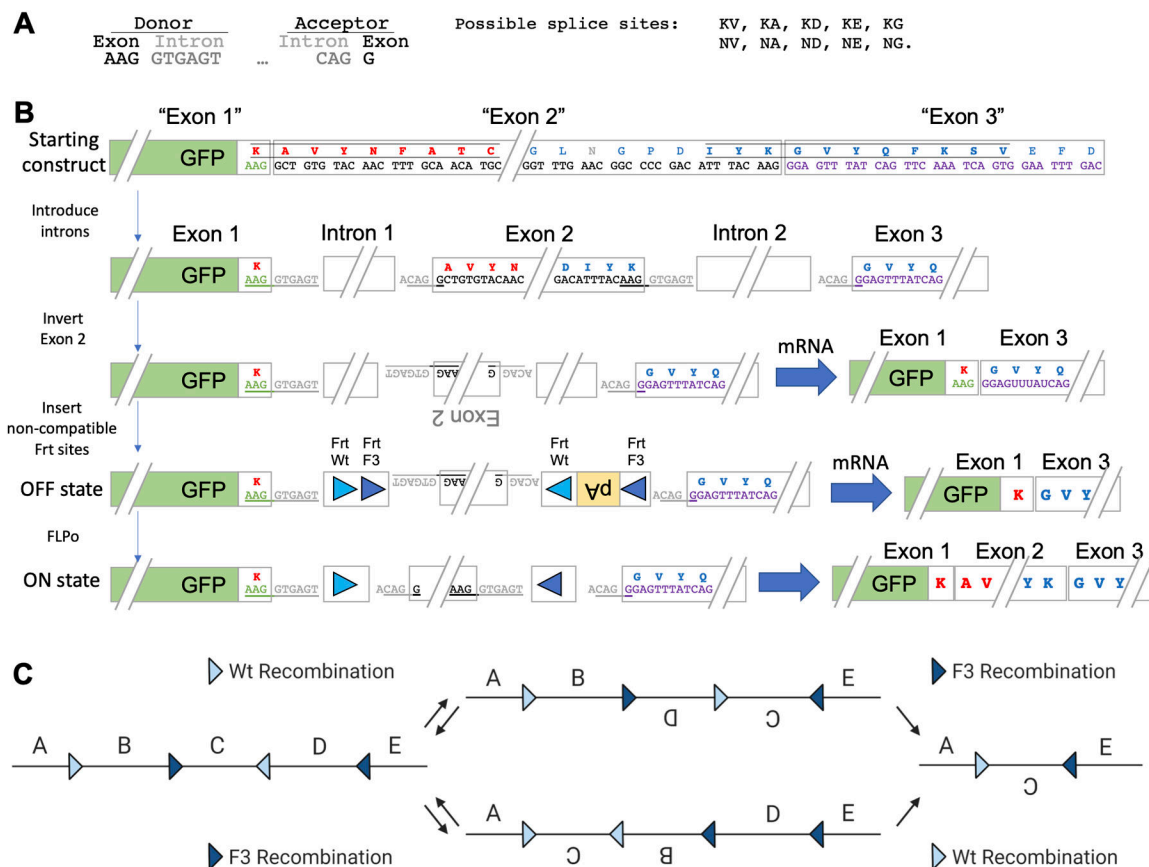
## Statistical analyses

All statistical analyses (paired and unpaired t tests) were performed using Prism V8.3.0 software.

## Figure Design

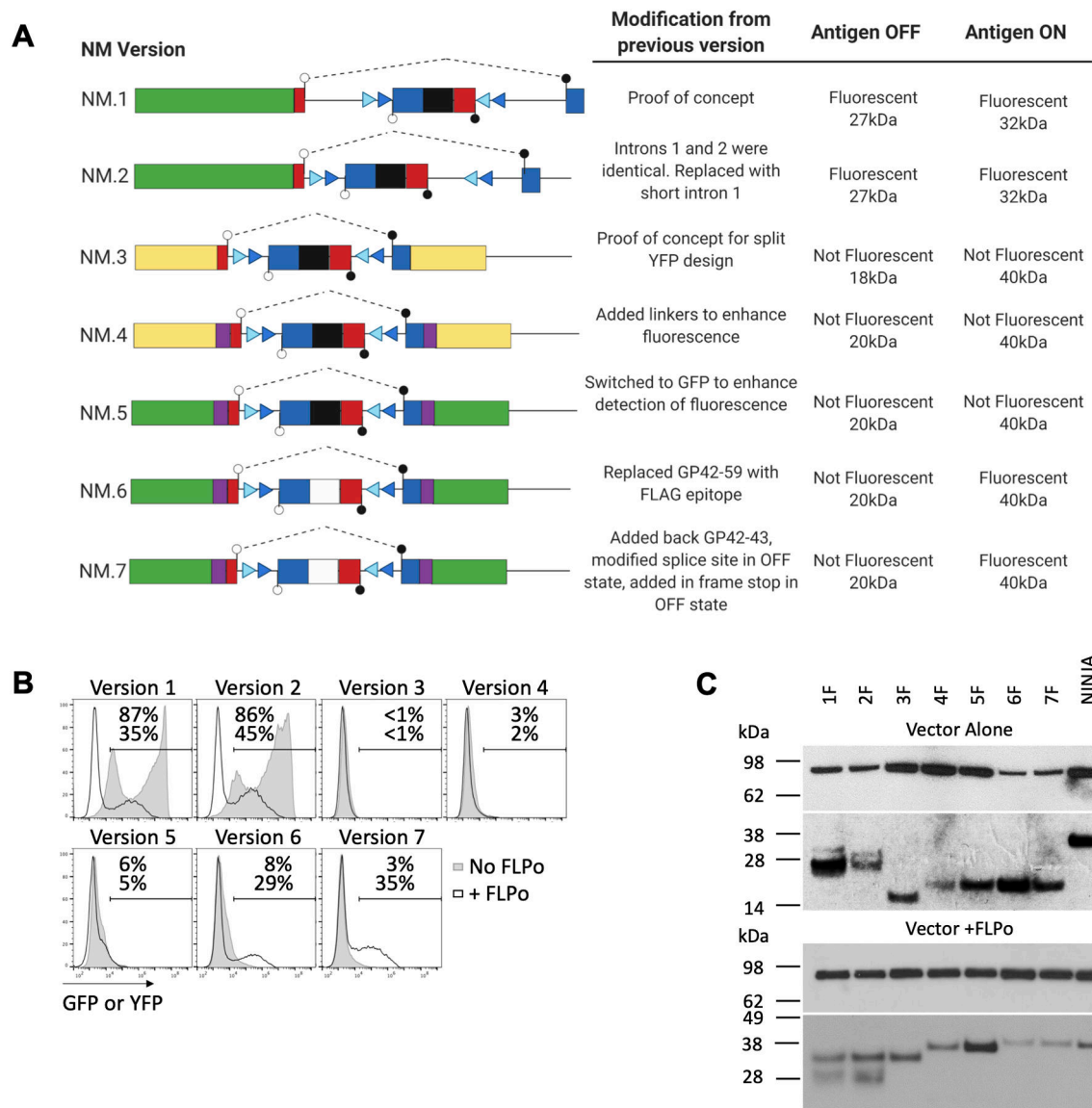
Figures 1a, 2a, and Extended Data Figure 5b were created with BioRender.

### Extended Data



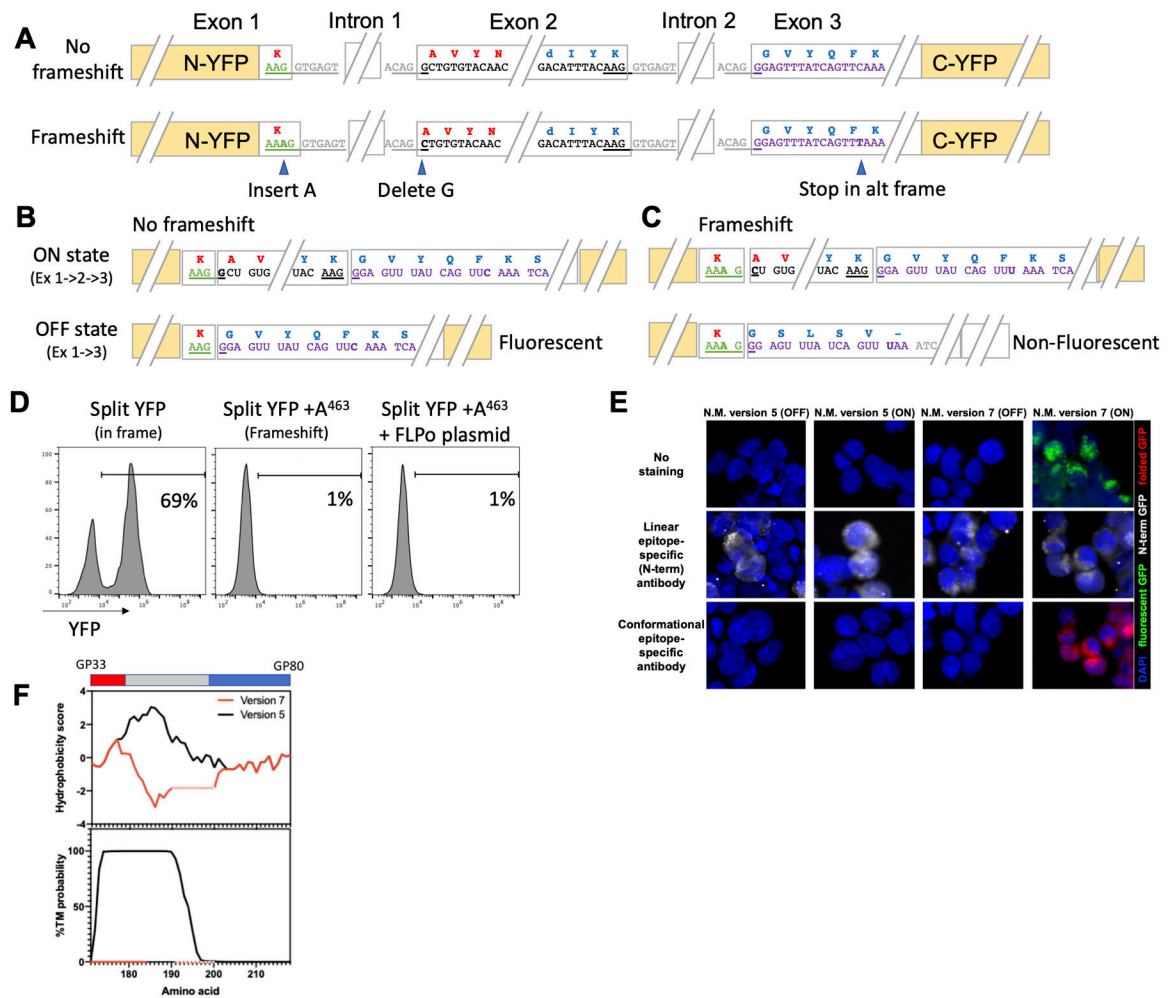
**Extended Data Figure 1 - Introduction of splice sites into NM**

**a**, Possible splice donor and acceptor sequence candidates in the NM to create Exon 2. **b**, Design and inversion of Exon 2, with transcription in OFF state resulting in splicing directly from Exon 1 to Exon 3. Insertion of non-compatible Frt sites shown in light and dark blue arrows. **c**, FLPo recombinase activity results in permanent inversion and transcription of all exons of the NM.



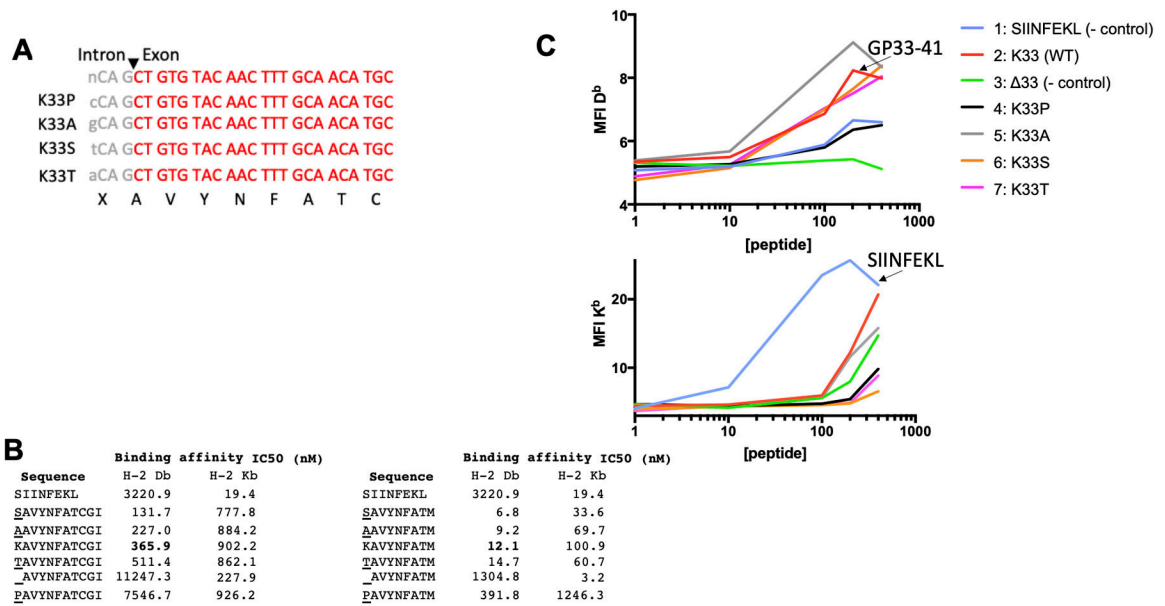
### Extended Data Figure 2 - Development of advanced versions of NM

**a.** Schematic shows 7 versions of the NM, with modifications made at each step and the fluorescence status at either ON or OFF state. **b.** Flow cytometry histograms of GFP or YFP fluorescence in each version, with or without FLPO activation. Representative of 3 independent experiments. **c.** Western blotting for GRP94 (control, top panel) or N-terminal GFP (bottom panel) on lysates from 293T cells transiently transfected with each version of NM, with (top blot) or without (bottom blot) FLPO. Positive control (+) is cell lysate from KP-C4A3D6 after FLPO. Representative of 3 independent experiments.

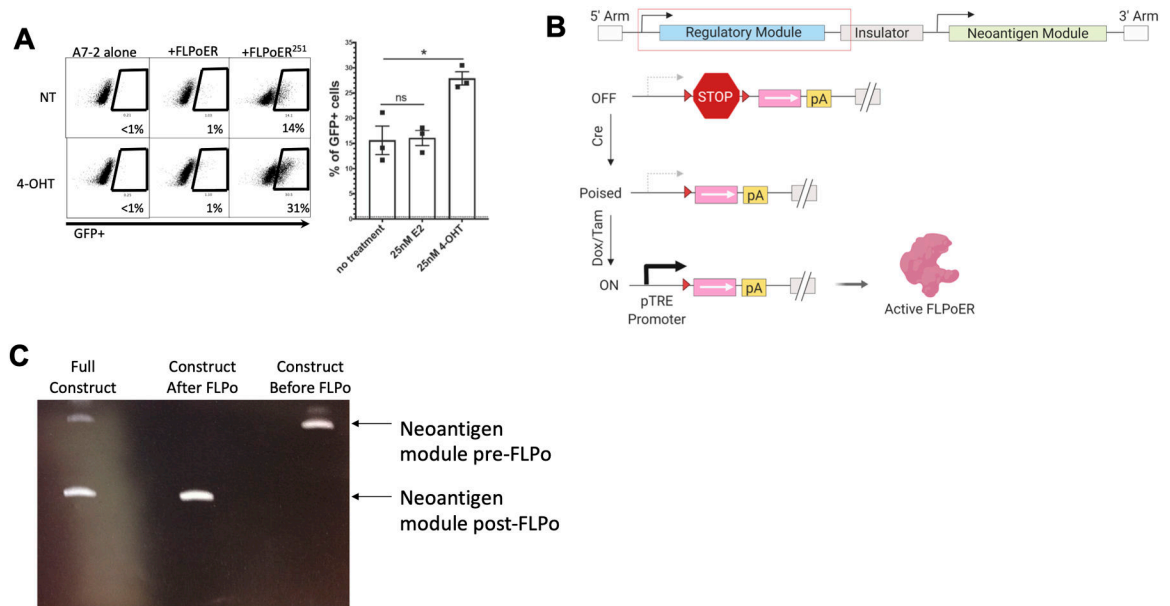


### Extended Data Figure 3 - Introduction of frameshift into NM

Schematic of NM.3, which shows the two possible *in silico* insertions of the spliced neoantigen construct from NM.2 in YFP, where in one skipping exon 2 results in a frameshift and premature stop codon. **b-c**, The transcription product and fluorescence status in the ON or OFF state is shown for the frameshift version (b) or no frameshift version (c). **d**, Flow cytometry histograms of YFP fluorescence of the constructs from c. The frameshift version is only YFP positive after FLPo exposure. Representative of 3 independent experiments. **e**, 293T cells transiently transfected with plasmids expressing the indicated version of the NINJA NM were imaged by confocal microscopy after staining with an antibody specific for either the N-term portion of GFP (middle panels), for a conformational epitope of GFP (bottom panels) or with no antibody (top panels). BLUE = DAPI, RED = folded GFP, GREEN = fluorescent GFP. Representative images are shown ( $n = 3$ ). **f**, Hydrophobicity score (top graph) in relation to amino acid position along the NM (red/grey/blue rectangle). In version NM.5 (black line) positions GP43-GP59 are predicted to be a transmembrane domain (bottom graph), and this elevated hydrophobicity is abrogated when replaced by a FLAG domain in NM.7 (red line).

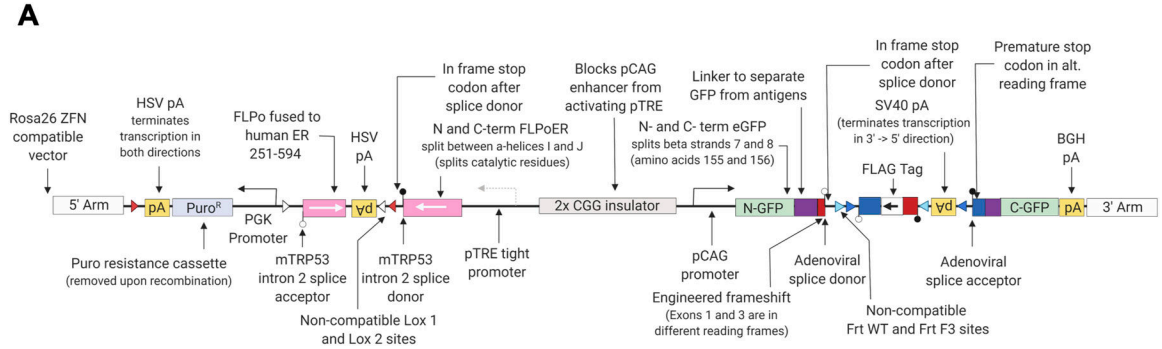


**Extended Data Figure 4 - Peptides from splice junction in NM are not presented as antigens**  
**a**, The antisense DNA sequence of exon 2 encodes GP34–41 with a preceding amino acid encoded by nCA, which could encode an Ala, Ser, Thr, or Pro residue **b**, the predicted binding of each peptide (SIINFEKL control, GP34–41, or GP33–41 with K33A, K33S, K33T, or K33P mutations). K33P did not bind to H2-D<sup>b</sup> or stimulate T cell activation.

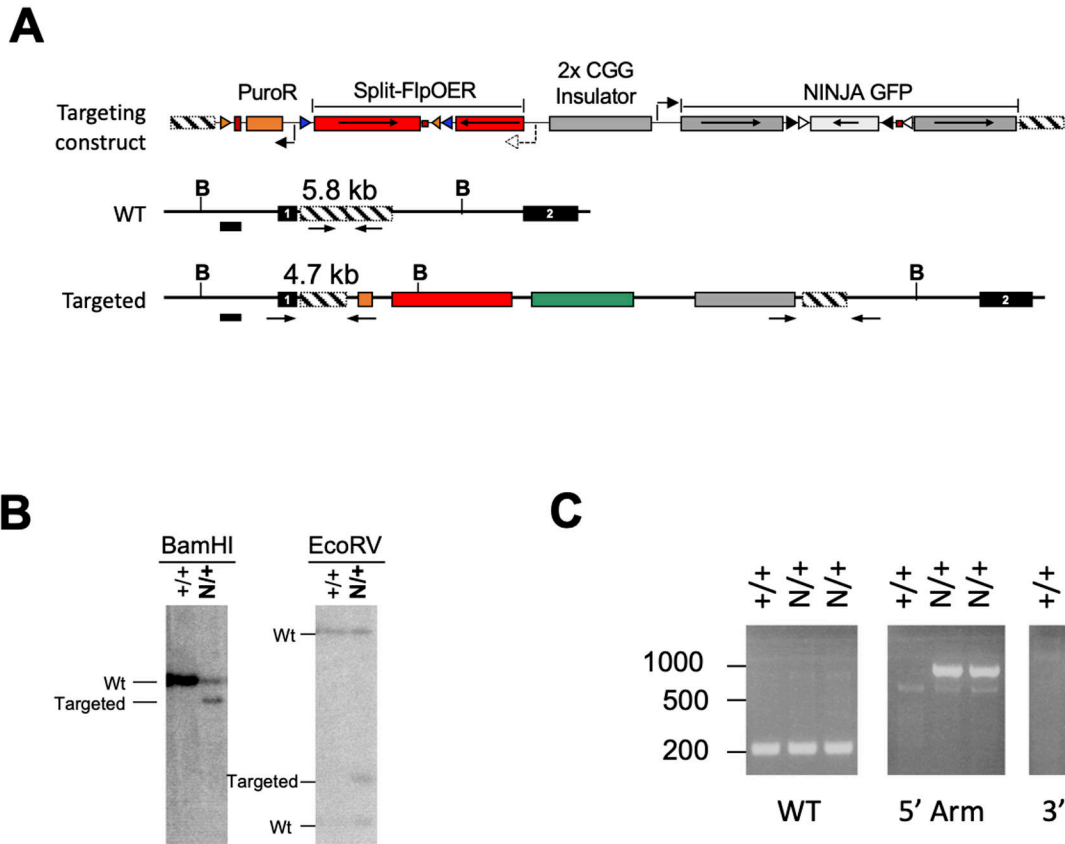


**Extended data Figure 5 - Design and development of RM**  
**a**, Flow cytometry plots of GFP expression in transiently transfected 293s with either NM.7 alone or in combination with FLPoER or FLPoER<sup>251</sup>. FLPoER<sup>251</sup>, while leakier, is more responsive to 4-OHT treatment than FLPoER and its activity was not increased by estrogen (E2) treatment. Data reflects n=3 technical replicates per group; 3 independent experiments.

(Unpaired two-tailed t tests, \*,  $P = 0.0170$ , ns,  $P = 0.896$ . Measure of centre for no treatment = 15.6(+/-2.8)%, for E2 = 16.1(+/-1.5)%, for 4-OHT = 27.9(+/-1/3% . Error bars = mean with SEM.) b, An early regulatory module design, with pTRE:Lox-STOP-Lox (LSL):FLPoER<sup>251</sup> 2x CGG insulator, and the NM. We discovered in c, that the NM in this construct was recombined by FLPo activity in *E coli*, which led to the later inverted design.

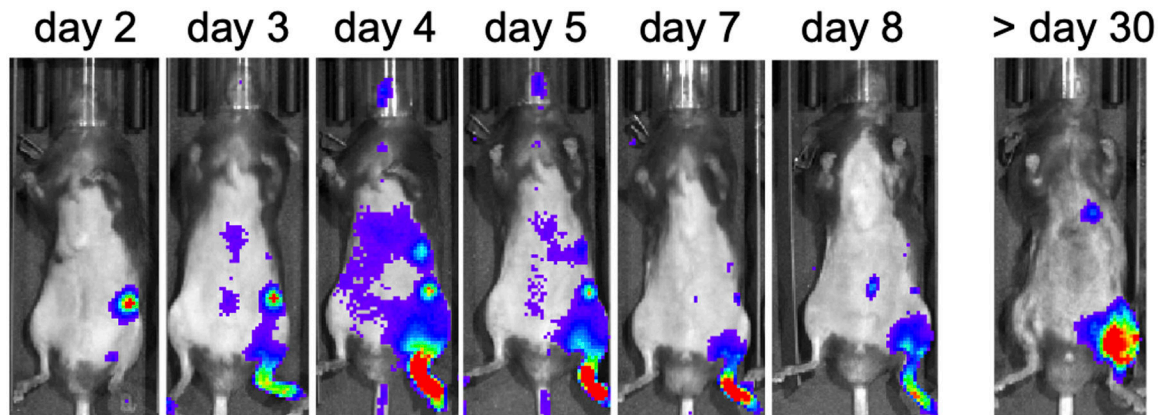


**Extended Data Figure 6 - Schematic diagram of completed NINJA construct**  
Final version of the NINJA construct, including the final RM and NM.

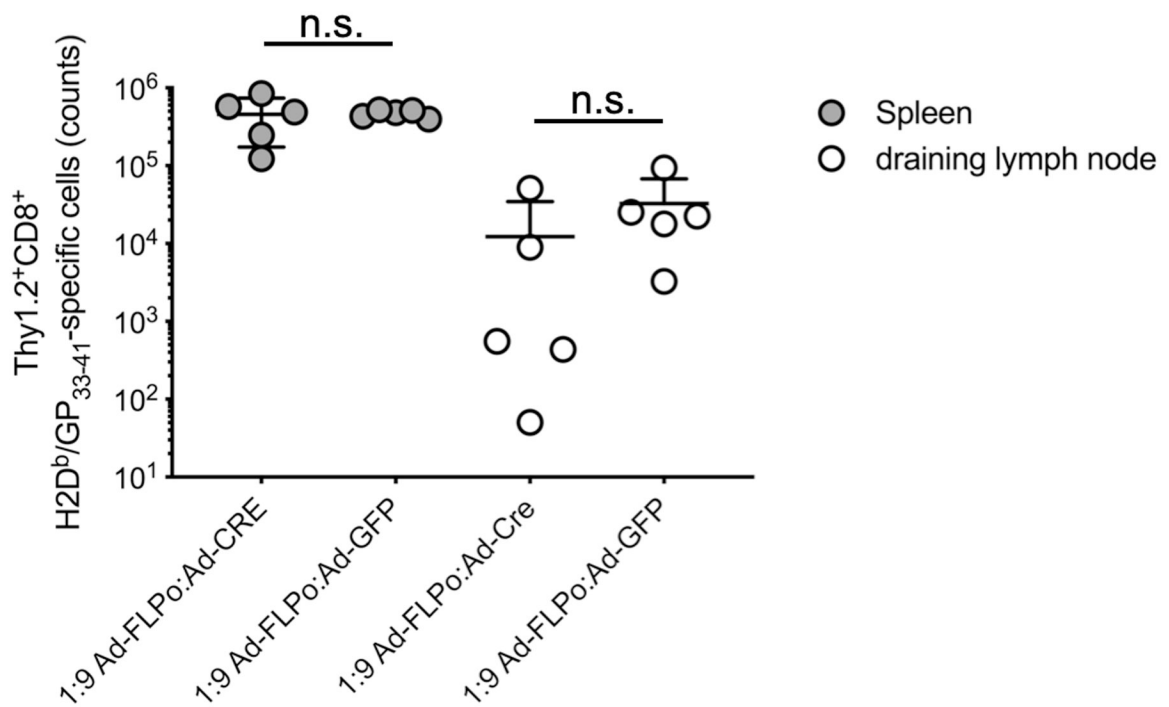


**Extended Data Figure 7 - Targeting of ES cell clones for NINJA**  
a, Schematic showing the Rosa 26 targeting construct used for generation of the NINJA mouse. b, Southern blotting confirmation of successful target insertion of NINJA. Single

experiment. **c**, Confirmation of germline transmission in two pups via PCR in the Rosa locus. Representative of >1000 experiments.

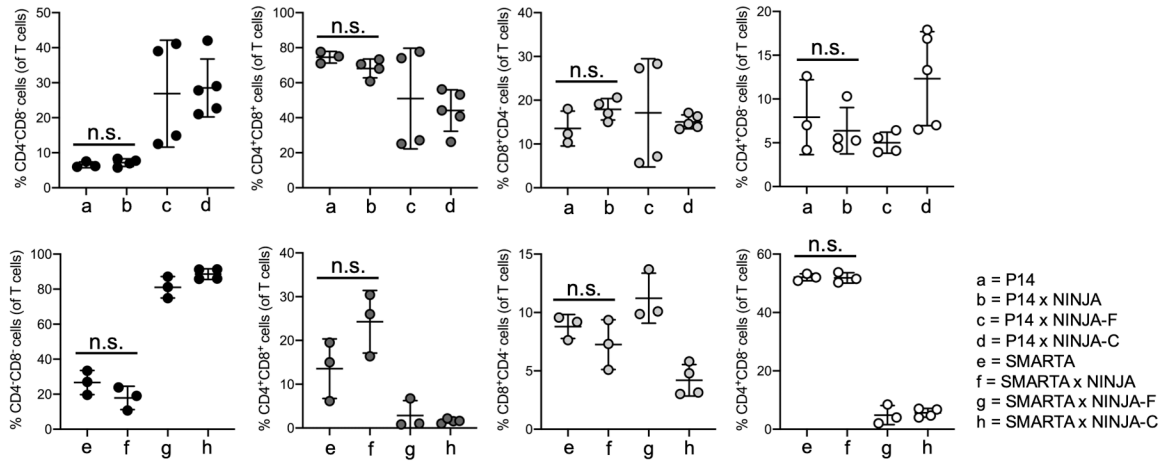


**Extended Data Figure 8 - Time course of neoantigen-specific CD8 T cell response in NINJA**  
Images show local accumulation and expansion of fLuc<sup>+</sup> P14 T cells adoptively transferred into NINJA mice that were subsequently infected S.C. in the footpad with Ad-FLPo ( $10^7$  PFU/mouse) and imaged by IVIS at the indicated day after infection. Representative mice are shown ( $n = 3$ ). Intensity of signal (blue to red) indicates accumulation of T cells.



**Extended Data Figure 9 - Ad-Cre infection does not lead to leaky neoantigen expression**  
Quantification of endogenous H2Db/GP<sub>33-43</sub>-specific Thy1.2<sup>+</sup>CD8<sup>+</sup> cells from the spleen (gray dots) and draining LNs (white dots) of NINJA mice 8 days after S.C. infection in the footpad with the indicated mixes of Ad-FLPo + Ad-Cre or Ad-FLPo + Ad-GFP (total dose  $10^7$  PFU/mouse) was performed by flow cytometry. Representative experiment is shown ( $n$

= 5). n.s. = difference not significant by two-tailed unpaired *t* test for comparisons of (Ad-FLPo + Ad-Cre) vs. (Ad-FLPo + Ad-GFP) responses in the spleen ( $P=0.9$ ) and in the draining LNs ( $P=0.3$ ). Average values  $\pm$  SD are shown.



### Extended Data Figure 10 - Analysis of thymic development in NINJA strains

Dot plots from Figure 3b show the average frequency  $\pm$  SD of each thymocyte population as determined by FC analysis for the indicated mouse strains (each dot represents one mouse,  $n=3$ , 2 experimental repeats). n.s., not significant by two-tailed unpaired *t* test ( $0.1 > P > 0.9$ ).

## Supplementary Material

Refer to Web version on PubMed Central for supplementary material.

## Acknowledgements

We thank Joshi lab members for reviewing the manuscript, and S. Jameson, J. Obhrai, and E. Sun for helpful discussions. We also thank the Yale Cancer Center (P30 CA016359 40), Yale Flow Cytometry Core, Yale School of Medicine Histology Facility, Dr. Peter Cresswell for confocal microscopy, the Swanson Biotechnology Center Preclinical Modeling facility of MIT for ES cell targeting, the University of Iowa Viral Vector Core for recombinant adenoviral vectors, Dr. Philippe Soriano for Ad-FLPo vector, and the NIH Tetramer Core Facility. This work was supported by grants from the Howard Hughes Medical Institute (T.J.), the K22 transition to Independence grant NCI-K22CA200912 (N.S.J.), the Damon Runyon Cancer Foundation (N.S.J.), The G. Harold & Leila Y. Mathers Foundation (N.S.J.), and the National Institute of Diabetes and Digestive and Kidney Diseases of the National Institutes of Health under Award Number P30KD034989 (N.S.J.). The content is solely the responsibility of the authors and does not necessarily represent the official views of the National Institutes of Health. T.J. is a Howard Hughes Investigator and a Daniel K. Ludwig Scholar.

## References

1. Curtsinger JM, Lins DC & Mescher MF Signal 3 determines tolerance versus full activation of naive CD8 T cells: dissociating proliferation and development of effector function. *J Exp Med* 197, 1141–1151 (2003). [PubMed: 12732656]
2. Harding FA, McArthur JG, Gross JA, Raulet DH & Allison JP CD28-mediated signalling co-stimulates murine T cells and prevents induction of anergy in T-cell clones. *Nature* 356, 607–609 (1992). [PubMed: 1313950]
3. Hugues S et al. Distinct T cell dynamics in lymph nodes during the induction of tolerance and immunity. *Nat Immunol* 5, 1235–1242 (2004). [PubMed: 15516925]
4. Iwasaki A & Medzhitov R Toll-like receptor control of the adaptive immune responses. *Nat Immunol* 5, 987–995 (2004). [PubMed: 15454922]

5. Joshi NS et al. Inflammation directs memory precursor and short-lived effector CD8(+) T cell fates via the graded expression of T-bet transcription factor. *Immunity* 27, 281–295 (2007). [PubMed: 17723218]
6. Cebula M et al. An inducible transgenic mouse model for immune mediated hepatitis showing clearance of antigen expressing hepatocytes by CD8+ T cells. *PLoS One* 8, e68720 (2013). [PubMed: 23869228]
7. Cheung AF, Dupage MJ, Dong HK, Chen J & Jacks T Regulated expression of a tumor-associated antigen reveals multiple levels of T-cell tolerance in a mouse model of lung cancer. *Cancer Res* 68, 9459–9468 (2008). [PubMed: 19010921]
8. Strandt H et al. Neoantigen Expression in Steady-State Langerhans Cells Induces CTL Tolerance. *J Immunol* 199, 1626–1634 (2017). [PubMed: 28739880]
9. Brockschneider D, Pechmann Y, Sonnenberg-Riethmacher E & Riethmacher D An improved mouse line for Cre-induced cell ablation due to diphtheria toxin A, expressed from the Rosa26 locus. *Genesis* 44, 322–327 (2006). [PubMed: 16791847]
10. Lee P et al. Conditional lineage ablation to model human diseases. *Proc Natl Acad Sci U S A* 95, 11371–11376 (1998). [PubMed: 9736743]
11. Malhotra D et al. Tolerance is established in polyclonal CD4(+) T cells by distinct mechanisms, according to self-peptide expression patterns. *Nat Immunol* 17, 187–195 (2016). [PubMed: 26726812]
12. Probst HC, Lagnel J, Kollias G & van den Broek M Inducible transgenic mice reveal resting dendritic cells as potent inducers of CD8+ T cell tolerance. *Immunity* 18, 713–720 (2003). [PubMed: 12753747]
13. Esterhazy D et al. Compartmentalized gut lymph node drainage dictates adaptive immune responses. *Nature* 569, 126–130 (2019). [PubMed: 30988509]
14. Luo X et al. ECDI-fixed allogeneic splenocytes induce donor-specific tolerance for long-term survival of islet transplants via two distinct mechanisms. *Proc Natl Acad Sci U S A* 105, 14527–14532 (2008). [PubMed: 18796615]
15. Kontos S, Kourtis IC, Dane KY & Hubbell JA Engineering antigens for in situ erythrocyte binding induces T-cell deletion. *Proc Natl Acad Sci U S A* 110, E60–68 (2013). [PubMed: 23248266]
16. Hlavaty KA et al. Tolerance induction using nanoparticles bearing HY peptides in bone marrow transplantation. *Biomaterials* 76, 1–10 (2016). [PubMed: 26513216]
17. Lutterotti A et al. Antigen-specific tolerance by autologous myelin peptide-coupled cells: a phase I trial in multiple sclerosis. *Sci Transl Med* 5, 188ra175 (2013).
18. Wilson DS et al. Synthetically glycosylated antigens induce antigen-specific tolerance and prevent the onset of diabetes. *Nat Biomed Eng* 3, 817–829 (2019). [PubMed: 31358881]
19. Hogquist KA, Baldwin TA & Jameson SC Central tolerance: learning self-control in the thymus. *Nat Rev Immunol* 5, 772–782 (2005). [PubMed: 16200080]
20. Anderson MS et al. Projection of an immunological self shadow within the thymus by the aire protein. *Science* 298, 1395–1401 (2002). [PubMed: 12376594]
21. Klein L, Roettinger B & Kyewski B Sampling of complementing self-antigen pools by thymic stromal cells maximizes the scope of central T cell tolerance. *Eur J Immunol* 31, 2476–2486 (2001). [PubMed: 11500832]
22. McGargill MA, Derbinski JM & Hogquist KA Receptor editing in developing T cells. *Nat Immunol* 1, 336–341 (2000). [PubMed: 11017106]
23. Ohashi PS et al. Ablation of “tolerance” and induction of diabetes by virus infection in viral antigen transgenic mice. *Cell* 65, 305–317 (1991). [PubMed: 1901764]
24. Zehn D & Bevan MJ T cells with low avidity for a tissue-restricted antigen routinely evade central and peripheral tolerance and cause autoimmunity. *Immunity* 25, 261–270 (2006). [PubMed: 16879996]
25. Kisielow P, Bluthmann H, Staerz UD, Steinmetz M & von Boehmer H Tolerance in T-cell-receptor transgenic mice involves deletion of nonmature CD4+8+ thymocytes. *Nature* 333, 742–746 (1988). [PubMed: 3260350]
26. Sha WC et al. Positive and negative selection of an antigen receptor on T cells in transgenic mice. *Nature* 336, 73–76 (1988). [PubMed: 3263574]

27. Miller JF & Flavell RA T-cell tolerance and autoimmunity in transgenic models of central and peripheral tolerance. *Curr Opin Immunol* 6, 892–899 (1994). [PubMed: 7710713]
28. Agudo J et al. GFP-specific CD8 T cells enable targeted cell depletion and visualization of T-cell interactions. *Nat Biotechnol* 33, 1287–1292 (2015). [PubMed: 26524661]
29. Schlake T & Bode J Use of mutated FLP recognition target (FRT) sites for the exchange of expression cassettes at defined chromosomal loci. *Biochemistry* 33, 12746–12751 (1994). [PubMed: 7947678]
30. Raymond CS & Soriano P ROSA26Flpo deleter mice promote efficient inversion of conditional gene traps in vivo. *Genesis* 48, 603–606 (2010). [PubMed: 20665730]
31. Schnutgen F et al. Enhanced gene trapping in mouse embryonic stem cells. *Nucleic Acids Res* 36, e133 (2008). [PubMed: 18812397]
32. Homann D et al. Mapping and restriction of a dominant viral CD4+ T cell core epitope by both MHC class I and MHC class II. *Virology* 363, 113–123 (2007). [PubMed: 17320138]
33. Mannering SI et al. The insulin A-chain epitope recognized by human T cells is posttranslationally modified. *J Exp Med* 202, 1191–1197 (2005). [PubMed: 16260488]
34. Skowera A et al. CTLs are targeted to kill beta cells in patients with type 1 diabetes through recognition of a glucose-regulated preproinsulin epitope. *J Clin Invest* 118, 3390–3402 (2008). [PubMed: 18802479]
35. Dunne JL, Overbergh L, Purcell AW & Mathieu C Posttranslational modifications of proteins in type 1 diabetes: the next step in finding the cure? *Diabetes* 61, 1907–1914 (2012). [PubMed: 22826307]
36. Carrillo-Vico A, Leech MD & Anderton SM Contribution of myelin autoantigen citrullination to T cell autoaggression in the central nervous system. *J Immunol* 184, 2839–2846 (2010). [PubMed: 20164413]
37. Dorum S et al. The preferred substrates for transglutaminase 2 in a complex wheat gluten digest are Peptide fragments harboring celiac disease T-cell epitopes. *PLoS One* 5, e14056 (2010). [PubMed: 21124911]
38. Grunewald J et al. Mechanistic studies of the immunochemical termination of self-tolerance with unnatural amino acids. *Proc Natl Acad Sci U S A* 106, 4337–4342 (2009). [PubMed: 19246393]
39. Myers LK et al. Relevance of posttranslational modifications for the arthritogenicity of type II collagen. *J Immunol* 172, 2970–2975 (2004). [PubMed: 14978100]
40. Kerppola TK Bimolecular fluorescence complementation (BiFC) analysis as a probe of protein interactions in living cells. *Annu Rev Biophys* 37, 465–487 (2008). [PubMed: 18573091]
41. Schrepf S, Froeschke M, Giroglou T, von Laer D & Dobberstein B Signal peptide requirements for lymphocytic choriomeningitis virus glycoprotein C maturation and virus infectivity. *J Virol* 81, 12515–12524 (2007). [PubMed: 17804515]
42. van der Most RG et al. Identification of Db- and Kb-restricted subdominant cytotoxic T-cell responses in lymphocytic choriomeningitis virus-infected mice. *Virology* 240, 158–167 (1998). [PubMed: 9448700]
43. Puglielli MT et al. In vivo selection of a lymphocytic choriomeningitis virus variant that affects recognition of the GP33–43 epitope by H-2Db but not H-2Kb. *J Virol* 75, 5099–5107 (2001). [PubMed: 11333891]
44. Feil R, Wagner J, Metzger D & Chambon P Regulation of Cre recombinase activity by mutated estrogen receptor ligand-binding domains. *Biochem Biophys Res Commun* 237, 752–757 (1997). [PubMed: 9299439]
45. Kaczmarczyk SJ & Green JE A single vector containing modified cre recombinase and LOX recombination sequences for inducible tissue-specific amplification of gene expression. *Nucleic Acids Res* 29, E56–56 (2001). [PubMed: 11410679]
46. Stern P et al. A system for Cre-regulated RNA interference in vivo. *Proc Natl Acad Sci U S A* 105, 13895–13900 (2008). [PubMed: 18779577]
47. Joshi NS et al. Regulatory T Cells in Tumor-Associated Tertiary Lymphoid Structures Suppress Anti-tumor T Cell Responses. *Immunity* 43, 579–590 (2015). [PubMed: 26341400]
48. Jackson EL et al. Analysis of lung tumor initiation and progression using conditional expression of oncogenic K-ras. *Genes Dev* 15, 3243–3248 (2001). [PubMed: 11751630]

49. DuPage M, Dooley AL & Jacks T Conditional mouse lung cancer models using adenoviral or lentiviral delivery of Cre recombinase. *Nat Protoc* 4, 1064–1072 (2009). [PubMed: 19561589]
50. Luche H, Weber O, Nageswara Rao T, Blum C & Fehling HJ Faithful activation of an extra-bright red fluorescent protein in “knock-in” Cre-reporter mice ideally suited for lineage tracing studies. *Eur J Immunol* 37, 43–53 (2007). [PubMed: 17171761]
51. Nielsen M et al. Reliable prediction of T-cell epitopes using neural networks with novel sequence representations. *Protein Sci* 12, 1007–1017 (2003). [PubMed: 12717023]
52. Andreatta M & Nielsen M Gapped sequence alignment using artificial neural networks: application to the MHC class I system. *Bioinformatics* 32, 511–517 (2016). [PubMed: 26515819]

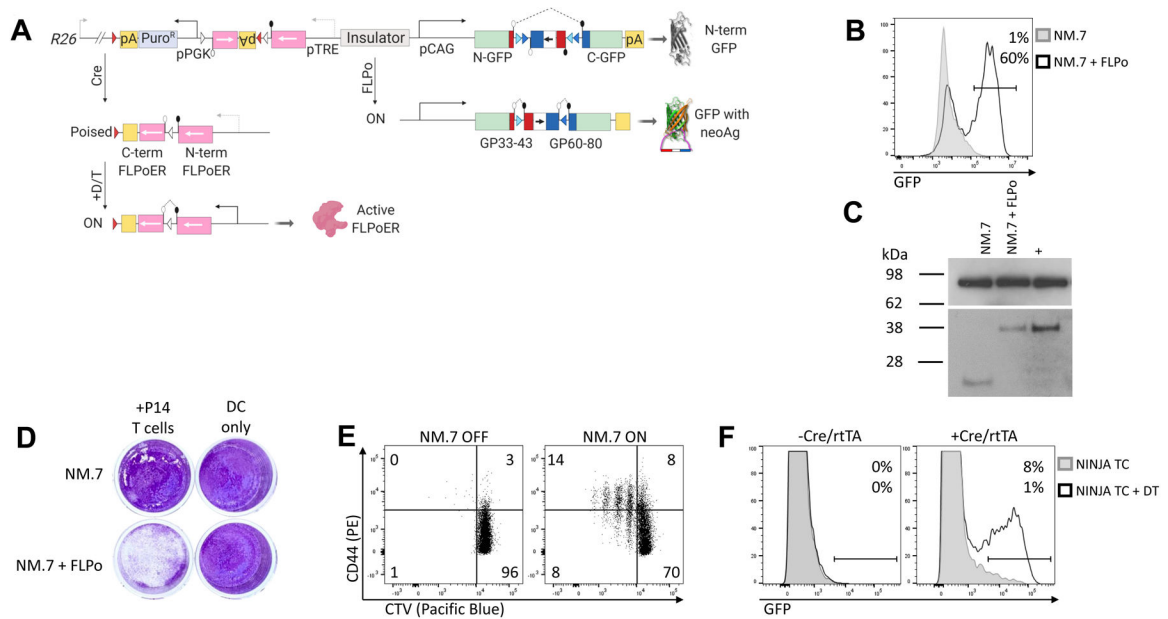


**Figure 1 - Design and development of NINJA targeting construct.**

Schematic of NINJA and transfections confirming fluorescence, protein size, T cell response, and D/T drug response. **a**, Schematic of NINJA targeting construct (NINJA TC) after integration into Rosa26 (R26) locus. NINJA contains regulatory (RM) and neoantigen (NM) modules. Schematic shows modules after Cre or FLPo recombinase and doxycycline/tamoxifen (D/T) exposure. (Red/ white fill arrow pairs = non-compatible loxP sites. Black/ white ball and stick lines = splice sites, and black/grey arrows = promoters. Light/dark blue fill arrow pairs = non-compatible FRT sites.) **b-c**, FLPo exposure is required for GFP expression from NM. 293T cells transfected with indicated constructs and assessed by FC or western blot. **b**, GFP expression 72 hours post-transfection with NM.7 alone (gray, filled) or NM.7+FLPo (line). % GFP+ is indicated. **c**, Western blotting for GRP94 (control, top panel) or N-terminal GFP (bottom panel) on cell lysates. Positive control (+) is KP-C4A3D6 after FLPo (see Figure 2). **d-e**, NM is only immunogenic after FLPo exposure. DC2.4 cells transfected with NM.7 or NM.7+FLPo and cultured +/- naive Cell Trace Violet (CTV)-stained P14 T cells. **d**, Tumor cells stained with crystal violet, day 4. **e**, CTV dilution and CD44 expression on CD8+ Va2+ T cells **f**, NINJA TC expresses GFP after Cre, rtTA, and D/T treatment. 293T cells were transfected with NINJA TC with and without plasmids expressing Cre and rtTA. Cells were then cultured with or without D/T. Histograms show GFP expression from the 293T cells with the indicated conditions. A-C, F Representative of 3 independent experiments, D-E single experiment.

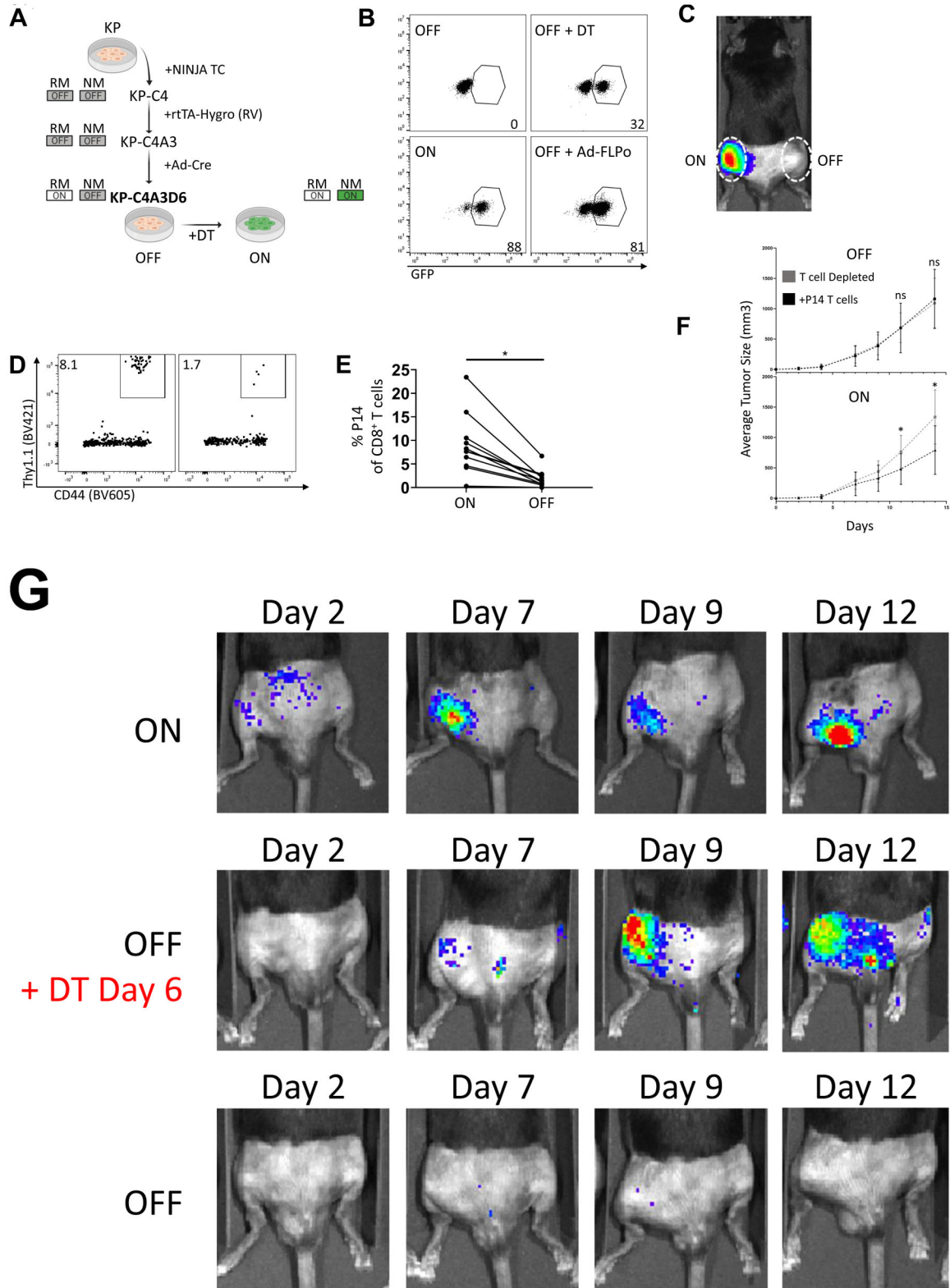
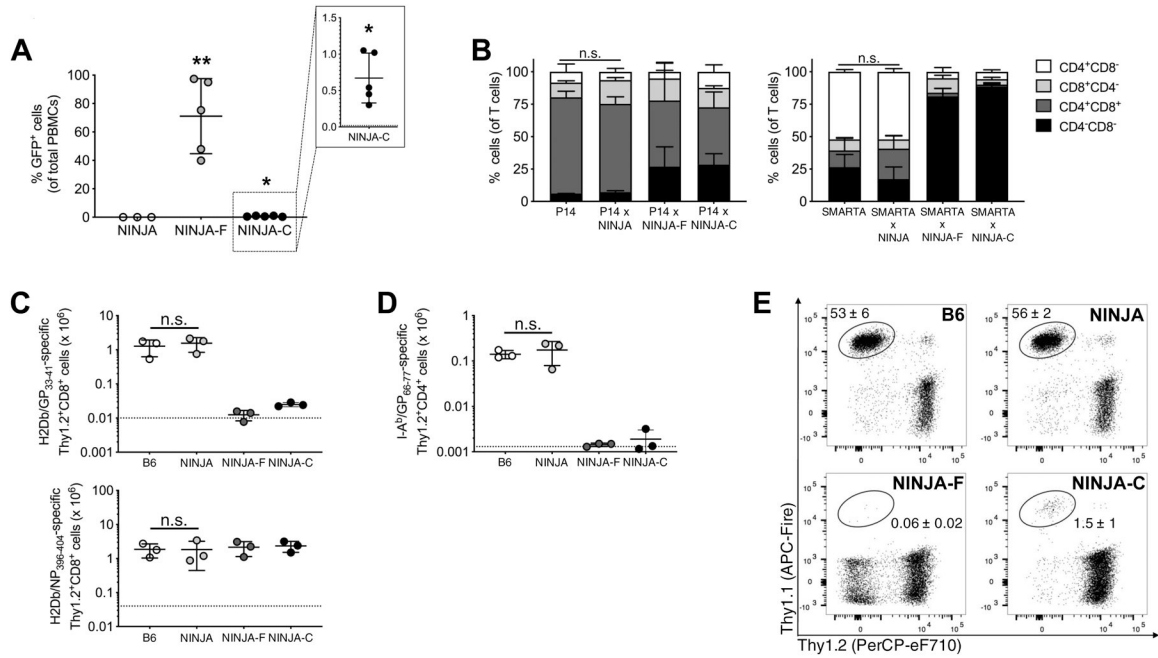
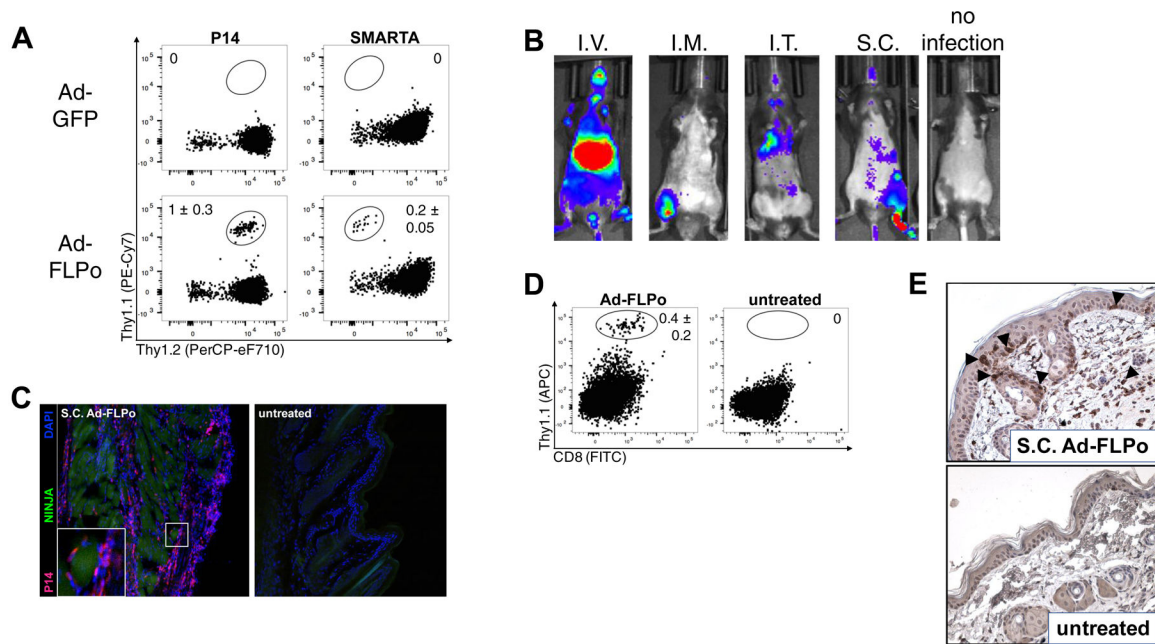


Figure 2 - NINJA cell line generates antigen specific T cell response following induction.

KP lung tumor cell line with poised NINJA turns on neontigens in response to D/T *in vitro* and *in vivo*. **a**, Schematic depicting generation of the “poised” KP-C4A3D6 cell line. **b**, GFP expression by untreated KP-C4A3D6 (OFF), or KP-C4A3D6 72 hours post-D/T treatment or Ad-FLPo. FC-sorted GFP+ KP-C4A3D6 cells shown as ON. **c-f**, KP-C4A3D6 cells only elicit tumor-specific CD8 T cell responses *in vivo* when ON. KP-C4A3D6 OFF and ON cells were intramuscularly transplanted bilaterally into B6 recipients ( $25\text{--}200 \times 10^3$  cells,  $n = 24$ ). Mice also received naive fLuc+ Thy1.1+ P14 T cells. **c**, Representative IVIS image shows signal from P14 T cells in ON and OFF tumors in the same mouse on day 11 after transplant. Intensity of signal (blue to red) indicates accumulation of T cells. **d**, FC dot plots pre-gated for CD8+ cells show presence of intratumoral Thy1.1+ CD44+ P14 T cells from ON and OFF tumor (numbers are average percent of  $n = 13$  in one experiment, plots are one representative mouse). **e**, Graph shows the frequency of intratumoral Thy1.1+ CD8+ P14 T cells from paired ON and OFF tumors (connected by line). (\*,  $P = 0.0006$  (paired t test, two tailed,  $n = 11$  co-injected animals)). **f**, Graph shows average tumor measurements of tumors in ON and OFF legs (\*,  $P < 0.0001$  in unpaired t test, two tailed; ns,  $P = 0.96$ ,  $P = 0.54$ . Minimum 3 experimental repeats; error bars are SD. ( $n = 29$ , +P14  $n = 36$  biologically independent animals)). **g**, *In vivo* activation of neoantigens triggers tumor-specific CD8 T cell response. KP-C4A3D6 OFF and ON cells were intramuscularly transplanted into B6 recipients that contained naive fLuc+ Thy1.1+ P14 T cells. IVIS images show signal from P14 T cells on indicated days. Intensity of signal (blue to red) indicates accumulation of T cells. Middle panels show treatment with D/T day 6–9 post-tumor inoculation. (2 independent experiments,  $n = 10/12$  treated animals responding).



**Figure 3 - Central and peripheral tolerance are bypassed in NINJA mice**  
**a**, No neoantigen expression at baseline in NINJA mice. Graph shows the frequency of NINJA-expressing GFP<sup>+</sup> peripheral blood mononuclear cells (PBMCs) isolated from NINJA, NINJA-F and NINJA-C mice (determined by flow cytometry). Dotted line represents background fluorescence signal from wild-type B6 PBMCs. Representative experiment ( $n = 3$ , 5 experimental repeats). Graph shows average values  $\pm$  SD. \*  $P = 0.02$  and \*\*  $P = 0.004$  by two-tailed unpaired  $t$  test for comparison of NINJA vs. NINJA-F or NINJA vs. NINJA-C. **b**, NINJA mice bypass central tolerance towards neoantigens. Bar graphs show the frequency of each gated thymocyte population determined by FC analysis for the indicated mouse strains ( $n = 3$ , 2 experimental repeats). Graph shows average values  $\pm$  SD. n.s., not significant by two-tailed unpaired  $t$  test ( $0.1 > P > 0.9$ ). Single dot plots are shown in Extended Data Figure 10. **c-d**, NINJA mice have normal CD8 and CD4 T cell responses to acute LCMV infection. Graphs showing the number of **c**, H2Db/GP<sub>33-41</sub>-specific (top) and H2Db/NP<sub>396-404</sub>-specific (bottom) Thy1.2<sup>+</sup>CD8<sup>+</sup> cells or **d**, I-A<sup>b</sup>/GP<sub>66-77</sub>-specific Thy1.2<sup>+</sup>CD4<sup>+</sup> cells from the spleen on day 8 after LCMV-Armstrong infection. Representative experiment ( $n = 3$ , 3 experimental repeats). Dotted lines represent background tetramer staining as determined on splenocytes from untreated B6. Graphs in **c-d** show average values  $\pm$  SD. n.s., not significant by two-tailed unpaired  $t$  test ( $0.5 > P > 1$ ). **e**, T cells are not tolerized by the peripheral environment of NINJA mice. Thy1.1<sup>+</sup>/1.1<sup>+</sup> P14 T cells were adoptively transferred into B6, NINJA, NINJA-F and NINJA-C mice. 2 weeks later, mice were infected with LCMV-Armstrong and analysis was conducted 8 days after infection. FC plots show the average frequency  $\pm$  SD of P14 CD8<sup>+</sup> T cells in the spleen ( $n = 6$ , 2 experimental repeats).



**Figure 4 - Expression and presentation of neoantigens after activation of the NM.**

**a.** Activation of neoantigen expression in NINJA BMDCs stimulates neoantigen-specific CD8 and CD4 T cell responses. BMDCs were generated from NINJA mice and infected with Ad-GFP (control, top) or Ad-FLPo (bottom) to turn on the NM directly. BMDCs were used to immunize B6 mice (subcutaneously, S.C.) that contained adoptively transferred Thy1.1<sup>+</sup>/1.2<sup>+</sup> P14 T cells and Thy1.1<sup>+</sup>/1.1<sup>+</sup> SMARTA T cells. Dot plots show average frequency  $\pm$  SD of P14 (left) or SMARTA (right) T cells from the indicated mice from a representative experiment ( $n = 11$ , 2 experimental repeats). **b.** Expansion of neoantigen-specific CD8 T cells is localized to the site of antigen induction. fLuc<sup>+</sup> Thy1.1<sup>+</sup> P14 T cells were adoptively transferred into NINJA mice that were subsequently infected intravenously (I.V.), intramuscularly (I.M.), intratracheally (I.T.) or S.C. (footpad) with Ad-FLPo. IVIS images show the location of P14 T cells 8 days after infection. Intensity of signal (blue to red) indicates accumulation of T cells. Representative mice are shown ( $n = 6$ , 2 experimental repeats). **c.** Neoantigen-specific T cells interact with neoantigen expressing skin cells after Ad-FLPo infection. dsRED<sup>+</sup> P14 T cells were adoptively transferred into NINJA mice that were subsequently infected with Ad-FLPo S.C. in the footpad (left) or left untreated (right). Confocal microscope images show GFP<sup>+</sup> NINJA-expressing cells (green), P14 T cells (red) and DAPI (blue) 8 days after infection. Representative images ( $n = 3$ ). **d-e.** Transgenic neoantigen-specific CD8 T cells respond to *in vivo* induction of neoantigens in the footpad. **d.** Dot plots show accumulation of Thy1.1<sup>+</sup> P14 T cells in the footpad of NINJA mice that were infected S.C. locally with Ad-FLPo 8 days before analysis. Representative mice are shown ( $n = 3$ , 2 experimental repeats). Average frequency and average MFI  $\pm$  SD are shown. **e.** Immunohistological sections of footpads from **d** show signs of immuno-mediated pathology indicated by epidermal/dermal thickening and infiltration by CD3<sup>+</sup> cells (arrows) in Ad-FLPo-infected samples but not in untreated samples. Representative images ( $n = 3$ ).

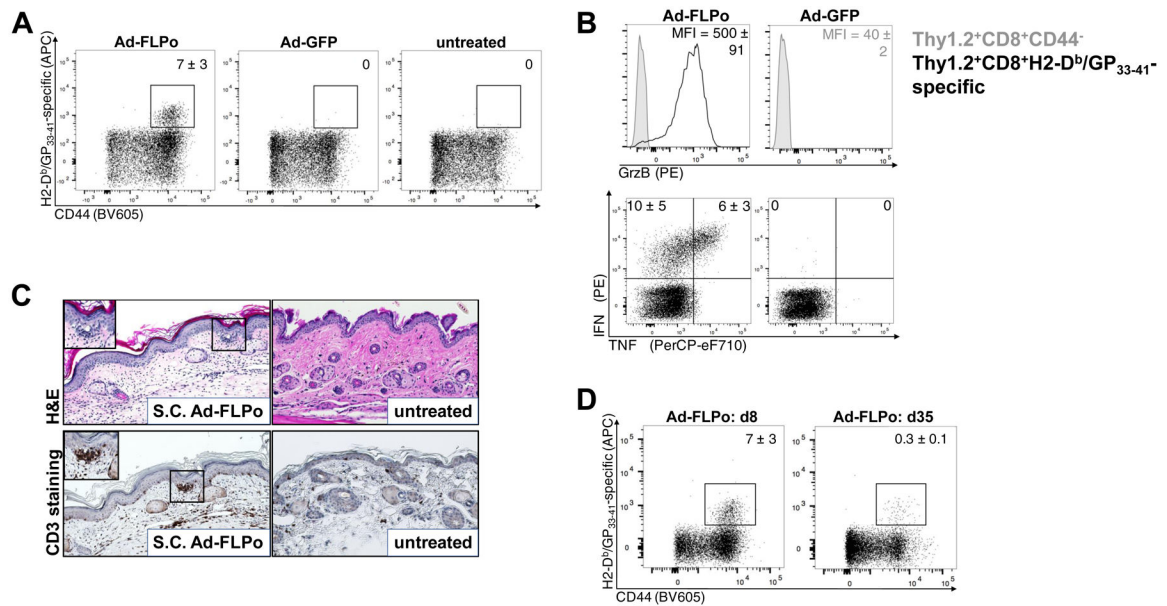


**Figure 5 - In vivo endogenous GP33-specific responses in NINJA mice after local infection with Ad-FLPo**

**a-c**, NINJA mice were left untreated or infected S.C. in the footpad with Ad-FLPo or Ad-GFP to analyze the development of endogenous neoantigen-specific effector CD8 T cell responses following local infection. **a**, FC plots show average frequency  $\pm$  SD of endogenous activated (CD44<sup>+</sup>) H2Db/GP<sub>33-43</sub>-specific Thy1.2<sup>+</sup>CD8<sup>+</sup> cells from the local draining LNs 8 days after infection. Representative dot plots are shown ( $n = 3$ , 3 experimental repeats). **b**, Histograms show Granzyme B expression (top) and FC plots show IFN $\gamma$  and TNF $\alpha$  production after *ex vivo* antigen-specific restimulation (bottom) by H2Db/GP<sub>33-43</sub>-specific Thy1.2<sup>+</sup>CD8<sup>+</sup> cells from **a**. Representative dot plots are shown ( $n = 3$ , 3 experimental repeats). Average frequencies and MFI  $\pm$  SD are indicated. **c**, Histological sections of footpad show epidermal and dermal thickening and infiltration by endogenous CD3<sup>+</sup> cells in NINJA mice infected S.C. with Ad-FLPo (top and bottom left) as compared to untreated NINJA mice (top and bottom right). Representative images ( $n = 3$ ). **d**, FC plots show average frequency  $\pm$  SD of endogenous CD44<sup>+</sup> H2Db/GP<sub>33-43</sub>-specific Thy1.2<sup>+</sup>CD8<sup>+</sup> cells from the local draining LNs 8 or 35 days after S.C. infection in the footpad with Ad-FLPo. Representative dot plots are shown ( $n = 4$ , 2 experimental repeats). MFI = mean fluorescence intensity; d = day.

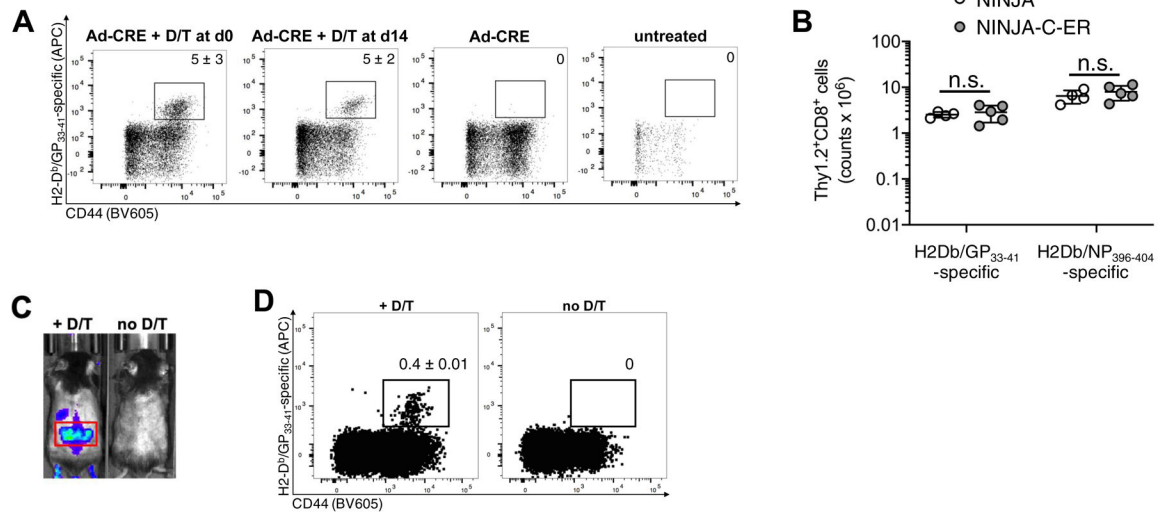


**Figure 6 - In vivo genetic tissue-specific activation of endogenous GP33-specific T cells**  
**a**, Temporally delayed antigen induction allows for neoantigen-specific CD8 T cell responses. FC plots show the average frequency  $\pm$  SD of endogenous activated (CD44<sup>+</sup>) H2Db/GP<sub>33-43</sub>-specific Thy1.2<sup>+</sup>CD8<sup>+</sup> cells from local draining LNs of NINJA mice 8 days after S.C. infection in the footpad with Ad-Cre alone (negative control) or Ad-Cre administered either together with D/T or 14 days prior to treatment with D/T. Representative dot plots ( $n = 4$ , 2 experimental repeats). **b**, NINJA-C-ER mice have normal CD8 and CD4 T cell responses to acute LCMV infection. Graphs show the number of H2Db/GP<sub>33-43</sub>-specific and H2Db/NP<sub>396-404</sub>-specific Thy1.2<sup>+</sup>CD8<sup>+</sup> splenocytes in the indicated strains 8 days after infection with LCMV-Armstrong ( $n = 5$ ). Average values  $\pm$  SD are shown. n.s., not significant by two tailed unpaired  $t$  test ( $P = 0.6$  for comparisons of H2Db/GP<sub>33-41</sub>-specific responses;  $P = 0.4$  for comparisons of H2Db/NP<sub>396-404</sub>-specific responses). **c**, fLuc<sup>+</sup> P14 T cells were adoptively transferred into NINJA-C-ER mice that were subsequently treated systemically with D and topically with T (painted on an area of the skin corresponding to the red square) or left untreated. IVIS images show local skin accumulation of P14 T cells only in the mice receiving D/T. Representative mice are shown ( $n = 3$ , 3 experimental repeats). **d**, Endogenous H2Db/GP<sub>33-43</sub>-specific Thy1.2<sup>+</sup>CD8<sup>+</sup> cells expand following local induction of neoantigen expression in the skin. Dot plots show average frequency  $\pm$  SD of H2Db/GP<sub>33-43</sub>-specific cells (pre-gated on Thy1.2<sup>+</sup>CD8<sup>+</sup> cells) in the local draining LNs of NINJA-C-ER mice 6 days after completing treatment with systemic D and topic T on a selected area of the skin. Representative mice are shown ( $n = 5$ ). D = doxycycline; T = 4-OHT.